Drought onset and propagation into soil moisture and grassland vegetation responses during the 2012-2019 major drought in Southern California

Maria Magdalena Warter[1], Michael Bliss Singer[1,2,3], Mark O. Cuthbert[1,2,4], Dar Roberts[5], Kelly K. Caylor[3,5,6], Romy Sabathier[1] and John Stella[7]

[1]School of Earth and Environmental Sciences, Cardiff University, Cardiff, CF10 3AT, United Kingdom
[2]Water Research Institute, Cardiff University, Cardiff, CF10 3AT, United Kingdom
[3]Earth Research Institute, University of California Santa Barbara, Santa Barbara, CA 93106-3060, USA
[4]Connected Waters Initiative Research Centre (CWI), School of Civil and Environmental Engineering, UNSW Sydney, NSW 2052, Australia
[5]Department of Geography, University of California Santa Barbara, Santa Barbara, CA 93117, , USA
[6]Bren School of Environmental Science and Management, University of California Santa Barbara, Santa Barbara, CA 93117, USA
[7]Department of Forest and Natural Resources Management, State University of New York College of Environmental Science and Forestry, Syracuse, NY 13210, USA

Correspondence to: Maria Magdalena Warter (warterm@cardiff.ac.uk)

Abstract

Despite clear signals of regional impacts of the recent severe drought in California, e.g., within Central Valley groundwater storage and Sierra Nevada forests, our understanding of how this drought affected soil moisture and vegetation responses in lowland grasslands is limited. In order to better understand the resulting vulnerability of these landscapes to fire and ecosystem degradation, we aimed to generalize drought-induced changes in subsurface soil moisture and to explore its effects within grassland ecosystems of Southern California. We used a high-resolution in situ dataset of climate and soil moisture from two grassland sites (coastal and inland), alongside greenness (NDVI) data from Landsat imagery to explore drought dynamics in environments with similar precipitation but contrasting evaporative demand over the period 2008-2019. We show that negative impacts of prolonged precipitation deficits on vegetation at the coastal site were buffered by fog and moderate temperatures. During the drought, the Santa Barbara region experienced an early onset of the dry season in mid-March instead of April, resulting in premature senescence of grasses by mid-April. We developed a parsimonious soil moisture balance model that captures dynamic vegetation-evapotranspiration feedbacks and analyzed the links between climate, soil moisture, and vegetation greenness over several years of simulated drought conditions, exploring the impacts of plausible climate change scenarios that reflect changes to precipitation amounts, their seasonal distribution, and evaporative demand. The redistribution

Deleted: Onset
Deleted: of drought
Deleted: Ocean
Deleted: decadal
Deleted: high-resolution
Deleted: . Analysis of data from
Deleted: to
Deleted: showed
Deleted: the
Deleted: net
Deleted: (netP)
Deleted: inlands
Deleted: at the coastal site.
Deleted: using netP-NDVI relationships as a leading indicator. We then…
Deleted: decadal timescales
Deleted: We found that all scenarios generate early, extreme soil moisture deficits during drought below a vegetation stress threshold, further intensifying early dry season onset and vegetation die-off. These changes suggest potential increases in the risk of wildfires in this and similar regions

of precipitation over a shortened rainy season highlighted a strong coupling of evapotranspiration to incoming precipitation at the coastal site, while the lower water holding capacity at the inland site resulted in additional drainage occurring under this scenario. The loss of spring rains due to a shortening of the rainy season also revealed a bigger impact on the inland site, suggesting less resilience to low moisture at a time when plant development is about to start. The results also suggest that the coastal site would suffer disproportionally from extended dry periods, effectively driving these areas into more extreme drought than previously seen. These sensitivities suggest potential future increases in the risk of wildfires under climate change, as well as increased grassland ecosystem vulnerability.

1 Introduction

The severe drought between 2012 and 2016 affected most of the state of California (USA), resulting in substantial impacts to water resources and ecosystems (NDMC, 2020; Prugh et al., 2018; Shukla et al., 2015; Williams et al., 2015), yet current understanding of the California drought's impacts is based on research within particular regions and biomes. Consecutive years of low precipitation, above average temperatures and extremely dry conditions (meteorological drought) over this drought period resulted in severely reduced snowpack, streamflow and groundwater storage (hydrological drought), periods of increased soil moisture deficit and elevated vegetative stress (agricultural drought), with dramatic effects on upland forest dieback and tree mortality (Berg et al., 2017; Diffenbaugh et al., 2015; Swain et al., 2014; Williams et al., 2015). Although, the entire state experienced drought effects to some degree, there were notable differences in vegetation responses between Northern and Southern California (Dong et al., 2019). In upland forests within the Sierra Nevada Mountains, there was large-scale canopy water loss and forest die-back as a result of the accumulated precipitation deficits, increased evaporative demand and soil moisture drying (Asner et al., 2016; Fettig et al., 2019; Goulden et al., 2019), while there were documented decline in vegetation greenness in Southern California (Dong et al., 2019). However, little is known about the propagation of drought from the atmosphere into soil moisture, and its associated effects on vegetation in lowland areas, especially within water-limited regions where grasses and shrubs dominate the landscape. These lowland, water-limited, grassland ecosystems exhibit complex relationships between vegetation and water availability that affect the spatial pattern and extent of different vegetation types, as well as the relative responses of different species to drought stress (Caylor et. al., 2006; Caylor et. al., 2009; D'Odorico et.al., 2007; Okin et. al., 2018). The progression of climate change and its potential impacts to the water balance demand a better understanding of how mean climate (temperature, precipitation) and soil water availability drive vegetation dynamics in lowland grasslands. The increasing loss of grassland ecosystems increases the threat of overall land degradation and encroachment of invasive species, which ultimately feeds back into heightened vulnerability of these ecosystems to water deficits under climate change (Gremer et al., 2015; Lian et al., 2020). In this study, we explore the links between climate, soil moisture, and vegetation during the recent California drought and analyze the potential consequences of future climate scenarios to advance our understanding of dynamic drought responses within vegetation in lowland grassland ecosystems.

Soil moisture is essential for plant growth and -health and accordingly, there are strong seasonal responses of vegetation to temperature and precipitation changes (Coates et al., 2015; Roberts et al., 2010). Grassland ecosystems throughout Southern California naturally exhibit green and senescent (brown) periods each year, due to the region's strong Mediterranean climate, which makes these ecosystems naturally fire prone during the dry season. Although such fires are part of the natural ecosystems of Southern California, they are also capable of encroaching on inhabited areas with disastrous effects (e.g., huge areas are

Deleted: A

Deleted: ,

Formatted: English (US)

Deleted: studies found

Deleted: ,

Deleted: during the drought

Deleted: whereas

Deleted: overall greater declines

Deleted: Little

Deleted: , however,

Deleted: impacts and

Deleted: through shallow

Deleted: the

Deleted: patterns

Deleted: However, as

Deleted: progress, there is

Deleted: need to

Deleted: understand

Deleted: furthers

Deleted: in semiarid landscapes

Deleted: Here

Deleted: further

Deleted: dynamics

Deleted: dryland

Deleted: Grassland ecosystems throughout Southern California naturally exhibit green and senescent (brown) periods each year, due to the region's strong Mediterranean climate, which makes these ecosystems prone to fire during the dry season.

Moved (insertion) [1]

Formatted: Font: 12 pt, Not Bold

Formatted: Font: Not Bold

currently burning due to fires spreading through grasslands in many Western states at the time of submitting this manuscript). Rising soil moisture deficits due to meteorological droughts can cause early senescence of vegetation, thus priming grasslands for intense wildfires, while also modifying species composition, runoff responses, and nutrient dynamics (Lian et al., 2020, Ludwig et al., 2005; McDowell et al., 2008; Michaelides et al., 2009). In recent decades, wildfire extent has increased substantially in Southern California, due to increased evaporative demand, reduced snowpack in mountainous areas and loss of dry season precipitation. Under these conditions native grasslands become more susceptible to non-native species invasion, and native sage scrub is lost (Singh and Meyer, 2020; Williams et al., 2019). The most destructive fires often occur at the end of the dry season when moisture content of live and dead fuels is severely reduced after months of warm and dry weather (Keeley et al. 2016; Williams et al., 2019). One example is the cascading effects of wildfire, subsequent rains, and debris flows that devastated Montecito in Santa Barbara County in 2018 (Oakley et al., 2018). Significant changes in rainfall intensity are expected around the globe (Trenberth, 2011; Westra et al., 2014), even in dryland areas (Singer & Michaelides, 2017; Singer et al., 2018), where we might expect drier spring and autumn periods, and an increase in subsequent dry years throughout many locations in California (Pierce et al., 2018). Such climatic conditions would likely further increase fuel aridity and wildfire potential, and lead to a shift in future fire regimes with more frequent and intense wildfires throughout the western US (Abatzoglou et al., 2016; Williams et al., 2019), thus potentially increasing the overall vulnerability of grasslands and surrounding communities.

Advances in remote sensing have provided new, spatially explicit observations of vegetation dynamics and moisture availability (Coates et al., 2015; Liu et al., 2012; Small et al., 2018). Additionally, the Food and Agriculture Organization (FAO) developed a well-established approach to estimate soil moisture for agricultural purposes (Allen et al, 1998), which has also proven to be useful for other non-agricultural applications (Cuthbert et al., 2013; Cuthbert et al., 2019). This simple soil moisture balance approach shows promise for understanding drought propagation into soil moisture. Soil moisture is our key drought metric of interest, as it inherently links precipitation, evaporative demand and Normalized Difference Vegetation Index (NDVI). The timing of vegetation growth and die-off is strongly related to seasonal fluctuations in water availability to plants, especially in annual grasslands, so the assessment of soil moisture and greenness is essential for vegetation drought monitoring (Liu et al., 2012; Small et al., 2018).

Currently, the vulnerability of California grasslands to future climate change is classified as 'moderately high', with some studies estimating a substantial loss of grassland habitats by the end of the 21st century (Thorne et al., 2016; Wilkening et al., 2019). The greater vulnerability of vegetation to drought in Southern California (compared to Northern California) and a continuing trend of aridification in this region will likely pose a compounding challenge to lowland vegetation and water

Deleted: making

Deleted: furthering the loss of

Deleted: , and conversion to invasive habitats throughout the region

Deleted: In Southern California, the spread of wildfires is further exacerbated by the Santa Ana winds, which can quickly promote fires across large areas, threatening residential communities and forest ecosystems (Williams et al., 2019). One example are

Deleted: Further warming trends are projected, leading to increasingly drier soil moisture conditions, increased precipitation variability and heightened evaporative demand. Under future climate change significant changes in rainfall intensity are expected throughout

Deleted: with

Moved down [2]: Currently, the vulnerability of California grasslands to future climate change is classified as 'moderately high', with some studies estimating a substantial loss of grassland habitats by the end of the 21st century (Thorne et al., 2016; Wilkening et al., 2019). The greater vulnerability of vegetation to drought in Southern California (compared to Northern California) and a continuing trend of aridification in this region will likely pose a compounding challenge to lowland vegetation and water resources throughout the entire US Southwest (Dong et al., 2019).

Formatted: Indent: First line: 0 cm

Deleted: Deep soil moisture drying has been shown to affect forest vegetation in uplands (Goulden et al., 2019). Grasslands are known to be highly sensitive to variations in precipitation and evaporative demand, which makes them particularly vulnerable to future climate change and shifts in precipitation variability (Gremer et al., 2015; Reynier et al., 2016).

Moved down [3]: Although many grass species are adapted to dry periods, a better understanding of the responses of lowland

Deleted: Higher temperatures and increased evaporative demand in the future may shift soil moisture conditions towards drier average

Moved down [4]: conditions, thereby increasing the risk of extreme droughts and stronger summer heatwaves (Ault et al., 2016,

Deleted: ¶

Deleted: has

Deleted: direct and indirect

Deleted: Proxy estimates of soil moisture, such as the Palmer Drought Severity Index (PDSI) or Standardized Precipitation ... [1]

Deleted: In this study we build upon the FAO approach by including dynamic interactions between vegetation and climate, ... [2]

Deleted: In this study we leverage these relationships to identify the responses of grassland vegetation to declining moisture ... [3]

Moved (insertion) [2]

resources throughout the entire US Southwest (Dong et al., 2019). Increases in temperatures and evaporative demand may shift soil moisture conditions towards drier conditions, thereby increasing the risk of extreme droughts and stronger summer heatwaves (Ault et al., 2016, Lian et al. 2020). Although many grass species are adapted to dry periods, a better understanding of the responses of lowland grassland vegetation to time-varying soil moisture stress associated with precipitation variability induced by climate change is essential to advance our knowledge and capabilities to mitigate the potential negative impacts of drought on these ecosystems.

In this study we build upon the FAO approach by including dynamic interactions between vegetation and climate through the incorporation of remotely sensed data to capture the relationship between soil moisture and vegetation, and use the model to investigate the evolution of soil moisture during the recent California drought and under several potential future drought scenarios. Our primary objective was to understand the broader patterns in the soil moisture and vegetation responses to climate forcing and to advance the understanding of how drought propagates through shallow soil moisture to affect lowland grassland vegetation. We investigated: (i) how local soil moisture evolved over the recent California drought; (ii) how changes in precipitation amounts and timing affected soil moisture dynamics and grassland vegetation; and (iii) how soil moisture might respond to more prolonged dry periods under plausible climate scenarios. We employed NDVI from Landsat alongside long-term, high resolution meteorological and soil moisture data from two distinct grassland locations in Santa Barbara County with contrasting climate conditions due to orography and air flow affecting evaporative demand: a coastal and an inland site. We used these data to parameterize a simple parsimonious single-layer soil moisture balance model for generalizing the impact of climate on plant available water in grassland ecosystems. We also developed a leading indicator of greenness based on available precipitation, which is used in our modeling framework to explore the effects of plausible climate change scenarios.

Moved (insertion) [4]

Moved (insertion) [3]

Deleted: and affects

Deleted: net

Deleted: that

Deleted: how

Deleted: would affect soil moisture and vegetation for this region in the future.

2 Data and Methods

2.1 Study Sites

In this study, we focused on two grasslands sites in Santa Barbara County in Southern California. The natural geography of this region is characterized by coastal plains, oak woodlands and a rugged mountain range (Roberts et al., 2010). Two sites were chosen from a network of several sites as they had the best data availability spanning over 10 years, while also representing the diverse geography of the region: a coastal grassland plain and an inland grassland site, north of the Santa Ynez Mountains (**Figure 1**). Both sites are characterized by a Mediterranean climate, with strongly seasonal precipitation during the winter and prolonged dry periods in the summer. The majority of precipitation falls between November and March, with an average of 352 mm (coastal) and 314 mm (inland) per water year (October-September). Previous studies have shown that growing season water availability strongly controls annual growth cycles and senescence of vegetation at these sites (Liu et al., 2012; Roberts et al., 2010).

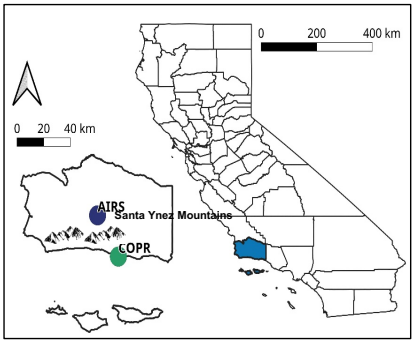

Figure 1: Location of stations in Santa Barbara County showing the coastal grassland site (COPR, green), with a marine microclimate and the semi-arid inland grassland site (AIRS, blue) north of the Santa Ynez mountain range.

The coastal site is the Coal Oil Point Reserve at an elevation of 6 mASL. The dominant vegetation at this site is classified as introduced European grassland with several non-native species, including a range of annual grasses and forbs. Species vary significantly between years, due to rainfall variability, however wild oat grass (*Avena fatua*) dominates the landscape. The

Moved up [1]: (Coates et al., 2015; Roberts et al., 2010).

Deleted: <*object*>Soil moisture is essential for plant growth and -health and accordingly, there are strong seasonal responses of vegetation to temperature and precipitation

Formatted: Font: 12 pt

Formatted: Font: 12 pt

Formatted: Font: 12 pt

Deleted: In this study

inland site is situated at Sedgwick Reserve Airstrip in the Santa Ynez Valley on the University of California's Sedgwick Natural Reserve at an elevation of 381 mASL. The site is an open grassland, and neither site is grazed. There is a higher species variability here than at the coastal site (mostly in the form of forbs) and includes several annual non-native grasses, such as various brome grasses (*Bromus hordeaceaus L., Bromus diandrus*) and also wild oat. The inland site is situated in a relatively dry valley in the rain shadow of the Santa Ynez mountain range, resulting in a higher evaporative demand during the summer due to higher temperatures (May-Aug average 28.5°C), compared to the coastal site (May-Aug average 20.6°C). Temperatures are more moderate at the coastal site, due to the presence of cooler, moister ocean air and coastal stratus clouds and thus lower insolation, enhanced by a coastal current, all of which reduce the overall evaporative demand (Roberts et al., 2010). The coastal and inland sites also vary in soil textural properties and water holding capacity, with soil types varying from clay loam at the coastal site to loam at the inland site, where there are distinctly higher sand contents (**Table S 1**). Soil samples from several depths were taken at the time of sensor installation in 2007 by University of California Santa Barbara (UCSB) and texture, porosity, field capacity and wilting point were determined in the lab.

2.2 Historical Climate

The United States Drought Monitor (USDM, https://droughtmonitor.unl.edu/) defines drought as a moisture deficit of such severity that it causes social, environmental, or economic effects. The USDM identifies and labels areas of drought within the United States based on a semi-quantitative intensity scale, derived from a combination of key indicators and information on soil moisture, precipitation, streamflow and drought severity, along with local condition and impact reports and ranges from D0 (Abnormally Dry) to D4 (Exceptional Drought) (NDMC, 2020). The recent multiyear drought affected the majority of the state of California between 2012-2016 (e.g., Dong et al., 2019) at varying levels according to the USDM (**Figure 2a**), whereas Santa Barbara County was under continuous drought conditions much longer (until 2019) (**Figure 2b**). The county was under 'extreme' (D3) to 'exceptional' (D4) drought from mid-2013 until early 2017, with the entire area remaining in the most severe category for several year. By spring 2017 the county was still under 'moderate' drought (D1), following a single wet winter season. However, the accumulated moisture deficit was so high after several years of exceptional drought conditions, that the state reverted to a state of 'severe' drought (D2) in 2018 after another abnormally dry year. The region finally came out of the drought completely in early 2019 after the wettest rainy season since 2005. Based on the drought designations from the USDM, we defined the following three drought categories: i) No drought (January 2010 - March 2012, February 2019 - October 2019 end of data), ii) Moderate Drought including periods of D0 and D1 and iii) Extreme Drought including periods of D2,D3 and

Deleted: This
Deleted: not used for grazing.
Deleted: in
Deleted: ,
Deleted: .
Deleted: ,
Deleted: .
Deleted: Soil types vary from clay loam at the coastal site to loam at the inland site, with distinctly higher sand contents at the inland site and a higher percentage of clay at the coastal site (**Table S 1**).
Deleted: **Data**¶
We used meteorological and soil moisture data from a network of several sites where data has been continuously recorded at 15-min resolution since 2007 by the University of California Santa Barbara for educational purposes (Roberts et al., 2010). The data are publicly available and continuously updated (http://www.geog.ucsb.edu/ideas/). Meteorological data from each station includes air temperature (T), relative humidity (RH), short wave and longwave radiation, wind speed and direction, and precipitation (P) among others. For each site, we extracted daily maximum daytime temperatures, humidity and precipitation totals ... [4]
Moved down [5]: at three different depths (10, 20 and 50 cm at
Deleted: For the purposes of this study we are using the shallowest ... [5]
Deleted:
Deleted: It
Deleted:). Based on the USDM,
Formatted: Font: Bold
Deleted: a lot
Deleted: : from 2012-
Deleted: .
Deleted: entire
Deleted: years (**Figure 2b**).
Deleted: of
Deleted: ,
Deleted: such
Deleted: these
Deleted: periods for our
Deleted: analysis in SB County: Non-
Deleted: (*PD*): 01-01-2008 to 31-12-2011
Deleted: (*D*): 01-01-2012 to 01-01-2019

D4. We apply the three different categories to characterize the meteorology of the drought and assess the changes in mean climate and vegetation responses.

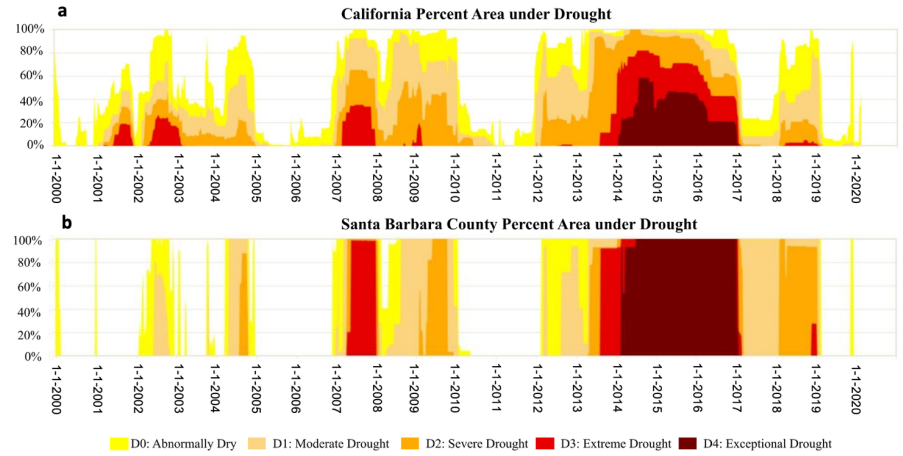

Figure 2: Timeseries of (a) percentage area of California under drought and (b) percentage area of Santa Barbara County under drought. [*The U.S. Drought Monitor is jointly produced by the National Drought Mitigation Center at the University of Nebraska-Lincoln, the United States Department of Agriculture, and the National Oceanic and Atmospheric Administration. Map courtesy of NDMC.*]

2 Deleted: 2.4 NDVI

We used meteorological and soil moisture data from a network of several sites where data has been continuously recorded at 15-min resolution since 2007 by UCSB for educational purposes (Roberts et al., 2010). The data are publicly available and continuously updated (https://ideas.geog.ucsb.edu/). Meteorological data from each station includes air temperature (T), relative humidity (RH), net radiation, wind speed and direction, and precipitation (P) among others. For each site, we summarized temperature and humidity to daily maximum daytime values and precipitation into daily totals to define the meteorology during our study period. We used other variables from the dataset, such as soil temperature, wind speed and net radiation to estimate the necessary parameters and calculate the reference evapotranspiration (ET_0) via the Penman Monteith

approach (Allen et al., 1998). We analyzed the date of onset (day of the year of last recorded precipitation for more than three months) and length of the dry season for each year and compared the timing between moderate drought, extreme drought, and non-drought periods. Two-sample Kolmogorov-Smirnov (KS) tests and/or Pearson's correlation were used to determine statistical differences between these periods, and to quantify correlations between variables, such as T, RH, P, PET, available P ($P - ET_0$ losses), soil moisture saturation, and Normalized Difference Vegetation Index (NDVI).

Volumetric soil water content and soil temperature were measured using in-situ probes (Stevens Hydro Probe II, Stevens Water Monitoring Systems Inc., Portland) at three different depths (10, 20 and 50 cm at the coastal and 15, 23 and 46 cm at the inland site) (Roberts et al., 2010). For the purposes of this study, we use the shallowest soil moisture at each site, in order to capture the precipitation and evapotranspiration dynamics of the shallow soil horizon we are investigating, which comprises the majority of the moisture availability to grasses. We present historical soil moisture as relative saturation levels, ranging from dry (0%) to fully saturated (100%), defined as the ratio of volumetric moisture content to the volume of pore space (porosity). This allows for a direct comparison of soil moisture between the two sites, considering the differing soil textural properties While the data recovery for both meteorological stations was continuous for the period of interest, the soil moisture probes at the inland site experienced significant data loss between 2016 – 2018, due to battery and sensor failure; these gaps in the data indicated in our results.

Moved (insertion) [5]

2.4 Normalized Difference Vegetation Index

Vegetation indices from remote sensing have been widely used to monitor the effects of drought on vegetation, as well as the links between precipitation, soil moisture, and plant sensitivity (Dong et al., 2019; Gu et al., 2008; Small et al., 2018). Multispectral indices, such as NDVI, provide good spatial and temporal representation of drought conditions, which can be combined with in situ measurement of soil moisture for a more detailed understanding of drought propagation and drought stress on vegetation (Gu et al., 2008; Okin et al., 2018). To analyze the seasonality and relationship between soil moisture and vegetation for our study period, we used NDVI images produced by the USGS from the surface reflectance using Landsat (Landsat-5 Thematic Mapper, Landsat-7 Enhanced Thematic Mapper and Landsat-8 Operational Land Imager), and which are produced every 16 days with a 30-m pixel resolution. Because we are using different Landsat instruments, the data from Landsat-5, 7 and 8 were homogenized after Goulden and Bales (2019), and all cloudy images were removed from the analysis using the pixel quality information provided by the U.S. Geological Survey with each image. We defined polygons around the measuring stations to capture a broader area of homogenous grassland vegetation and soil textural properties at the coastal (19,800 m^2) and inland site (35,100 m^2). The polygons are based on field surveys made during site installation and on direct analysis of homogenous NDVI images where everything was green and included only grassland vegetation (no trees). We

Deleted: Normalized Difference Vegetation Index (

Deleted:),

Deleted: derived

Deleted:) to analyze the responses of grasslands to the multi-year drought in Southern California. Landsat provides images every 16 days with a 30-m pixel resolution. We defined polygons around the measuring stations to represent

quantified spatially-averaged NDVI over each polygon to obtain a monthly time series for the period January 2008 to October 2019. NDVI, as a function of the red and near-infrared wavelengths, ranges from +1 to -1 and reaches its maximum (saturated) value of 1 in conditions of high plant vigor and photosynthetic activity, most common in forested areas and cultivated fields. Low or negative values are more representative of bare ground, senescent vegetation or water surfaces (Gillespie et al., 2018). Through a pixel-wise visual analysis of NDVI and comparison of different cover types (grassland, bare ground, forest, water) over our grassland sites, we established that in our study area green grassland vegetation is generally represented by values >0.3, while NDVI values <0.3 are more indicative of brown or senescent (non-photosynthesizing) vegetation.

2.5 Soil Moisture Balance Model

2.5.1 Model Description

We developed a simple, parsimonious model to better understand the linkages between climate, plant water availability and plant health and include experimental manipulations of climate variables to explore plausible future climate scenarios. Rather than attempting to model detailed soil moisture processes, we used a simplified soil moisture balance model (SMBM) established by the FAO, which is based on a 'bucket' approach (Allen et al., 1998), and is a variant of a code previously developed for estimating groundwater recharge (Cuthbert et al., 2013; 2019). Simple modeling frameworks capable of linking vegetation to water availability can be useful tools to assess past and future ecohydrological dynamics in a range of water-

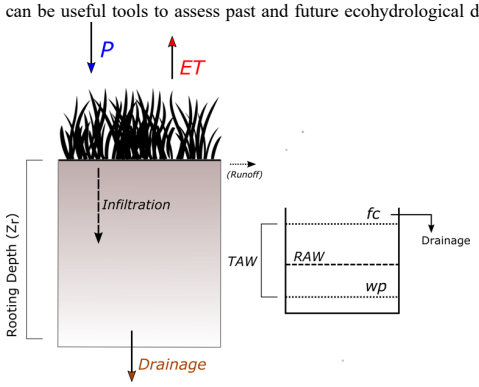

Figure 3: Simple conceptual design of a homogenous soil columns with of incoming and outoging fluxes and relevant soil parameters defining the amount of available water.

Deleted: create
Deleted: using median values of all pixels for each location
Deleted: visible
Deleted: .
Deleted: Page Break
Deleted: To characterize the effects of the recent California drought on soil moisture, we
Deleted: that enabled us
Deleted: allowed for
Deleted:),
Deleted: simple
Deleted: established by the FAO

limited environments (Caylor et al., 2009; D'Odorico et al., 2007; Evans et al., 2018; Quichimbo et al., 2020). Therefore, model inputs are kept as simple as possible and include information on soil properties, vegetation cover and climate (precipitation and the meteorological variables required to estimate potential evapotranspiration (PET). Due to the flat topography of our study sites, we assume runoff is zero, thus precipitation is either infiltrating into the soil or returned to the atmosphere through evapotranspiration. Figure 3 shows a simplified conceptual design of a homogenous soil column and the relevant incoming (P) and outgoing (ET, runoff and drainage) fluxes, as established by Allen et al. (1998). The model uses the concepts of total available water (TAW) and readily available water (RAW), which are dependent on soil textural properties, to estimate the soil moisture deficit and by extension soil moisture content. Runoff is assumed to be zero in our study, since our sites are located on flat ground. For this study, information on soil properties was available (**Table S1**), however if field measurements are unavailable typical ranges for field capacity, wilting point, and rooting depths can also be found in the FAO56 Manual (Tables 19 and 22 in Allen et al., 1998). The depletion fraction factor (*pc*) that decreases TAW is generally dependent on vegetation/crop type and was set to a commonly used range between 0.2-0.6 (Allen et al., 1998, Table 22). The SMBM was driven by precipitation from meteorological data and reference evapotranspiration estimated through Penman-Monteith, using meteorological data from the weather stations. Due to the richness of the IDEAS dataset, variables such as soil temperature, wind speed and net radiation were available, which allowed us to estimate the necessary parameters such as ground heat flux and conductance, to apply the Penman-Monteith model. Additional parameters in the SMBM are shown in **Table S2**.

2.5.3 Dynamic Vegetation Response

Within the SMBM actual evapotranspiration (AET) is estimated using a crop coefficient (k_c) as the empirical ratio relating plant ET to a calculated reference ET (ET_0) and to account for changes in evaporative demand over a growing season. Previous studies have explored the relationship between multispectral vegetation indices, such as NDVI, and crop coefficients, and have applied it successfully to estimate k_c at the field scale for different locations and climate conditions (Glenn et al., 2011; Hunsaker et al., 2005). Since k_c traditionally does not account for variations in plant growth due to climate variations or uneven water distribution, the alternative use of vegetation indices allows for a more accurate and dynamic estimation of ET (Nagler et al., 2005). NDVI was found to be closely correlated to ET, where maximum ET and maximum NDVI coincide at approximately the same time during a growing season, thus making NDVI a suitable proxy to estimate crop coefficients (Glenn et al., 2011) We use the same linear relationship between NDVI and k_c to model a temporally varying crop coefficient derived from vegetation indices to quantify plant ET as follows:

$$kc_{VI} = (VI *)^{\eta} \quad \textbf{(1)}$$

Deleted: Model inputs

Deleted:) (**Figure 3**

Deleted: ¶
The SMBM calculates a soil moisture deficit for a homogenous soil column of a certain rooting depth, which can be converted to vertically averaged, volumetric soil moisture content (m^3/m^3). The initial amount of available water to plants is defined by the water content at plant wilting point (θ_{wp} [m^3/m^3]), the effective field capacity (θ_{fc} [m^3/m^3]), and a certain rooting depth (Z_r [mm]). Rooting depth is based on the dominant crop and was taken from Allen et al. (1998, Table 22) based on the dominant vegetation at the study sites. The corresponding relevant quantities of water available to plants are characterized as Total Available Water and Readily Available Water. Total available water represents the amount of water a crop can extract from the root zone, depending on soil textural properties and rooting depth, while the readily available water represents a depleted fraction of the total available water that can be extracted from the root zone without the plants suffering from water stress. If the moisture deficit in the soil exceeds readily available amount, evaporation is adjusted through a water stress coefficient (k_s). As the water content gradually decreases through evapotranspiration following a rain event, the soil moisture deficit will increase. If no additional moisture is added through more precipitation, soil water content will reach its minimum value at wilting point, where no water is left for evapotranspiration and k_s becomes zero. The moisture deficit has reached its maximum value as the total available amount of water is exhausted. Following a heavy precipitation event, downward drainage (percolation) of water from the topsoil is occurring. No drainage occurs if the soil water content in the evaporation layer is below field capacity. A schematic overview of the key model parameters and the equations can be found in the Supplementary Material (**Figure S1**). ¶
For this study, we had information on soil properties available (**Table S 1**

Deleted: the total available amount of water

Deleted:

Deleted: potential

Deleted: (PET [mm/d]) was

Deleted: Other key

Deleted: 1.

Deleted: The FAO approach provides different methods for quantifying actual evapotranspiration (AET) for agricultural crops. In this study we used a time varying (dynamic) crop coefficient (k_c), which allows for variations in soil evaporation and plant transpiration. It is therefore meant to represent the dynamics of vegetation and ground cover during the growing season, from initial emergence to full plant maturation to senescence. As vegetation ... [6]

Deleted: Previous studies have explored the relationship between multispectral indices, such as NDVI and crop coefficients, and have applied it successfully to estimate k_c at the field scale for different locations and climate conditions (Hunsaker et al., 2005; Kamble et ... [7]

where kc_{VI} represents a plant transpiration coefficient, η is an exponent determined by the relationship of ET_0 as measured by Pearson's correlation, and the vegetation index used in Eq. 2. VI* is the vegetation index normalized between 0 and 1 to represent bare soil/dead vegetation and fully transpiring and unstressed vegetation respectively, and calculated as:

$$VI* = 1 - \frac{NDVI_{max} - NDVI}{NDVI_{max} - NDVI_{min}} \quad (2)$$

where $NDVI_{max}$ is the value when ET is maximal and $NDVI_{min}$ the ET of bare soil. Potential evapotranspiration can then be estimated as:

$$PET = ET_0 * kc_{VI} \quad (3)$$

where the estimated PET is used as a model input to quantify actual evapotranspiration (AET) within the SMBM.

2.5.4 Model Implementation

The data were separated into calibration and validation sets and model performance in each period was evaluated for acceptance or rejection of models. During calibration, model performance was optimized using data from January 01, 2008 to December 31, 2014. This time frame was chosen to include the natural variation of soil moisture dynamics, including non-drought and drought period. The model was then tested against data from January 01, 2015 to September 30, 2019. This period also includes natural variations in soil moisture, including the drought, individual very wet and dry years to account for the possibility of different combinations of parameter values that may all be equally successful at reproducing the observed soil moisture data. We defined the quantitative measures of acceptance/rejection criteria using Kolmogorov-Smirnov (goodness of fit) testing to identify parameter combinations that achieve statistically similar ($p > 0.01$) distributions in observed versus simulated soil moisture. The temporal dynamics of soil moisture were evaluated via Nash Sutcliffe Efficiency (NSE) to identify parameter combinations that adequately simulated the observed soil moisture series ($NSE > 0.5$). The models accepted during calibration and validation periods were then evaluated via goodness-of-fit and the best model and its parameters was used for simulating soil moisture under simple climate change scenarios. We developed an envelope of uncertainty based on Monte Carlo sampling (1000 simulations from a uniform distribution) using known ranges for soil textural properties and general estimates from Allen et al., (1998, Table 22) for rooting depth and depletion fraction and included ±1 standard deviation of all accepted models in the results to show the range of working models.

Deleted: Data for the period from January 01, 2008 to September 30, 2019 were used to calibrate the model. The range of estimates of SMBM parameters were constrained based on field measurements of soil texture (**Table S1**) and general estimates (rooting depth, Table 22 in Allen et al., 1998). We developed an envelope of uncertainty based on Monte Carlo sampling (1000 simulations from a uniform distribution) from these ranges.

Deleted: . Thus, we

Deleted: .

Deleted: We also

2.5.5 Representing Future Drought Scenarios

Projections of future climate change in California suggest that there will be shifts in precipitation frequency and variability during the dry season, with an increased number of dry days and increased evaporative demand, thus partly offsetting any increases in winter precipitation, and possibly shifting towards more extreme events (Aghakouchak et al., 2018; Berg & Hall, 2015; Cook et al., 2015; Pierce et al., 2018). A rise in temperature is expected throughout the Southwest and across the entire continent (Diffenbaugh et al., 2015). Furthermore, trends in emissions for California point towards a higher emissions scenario of RCP 8.5, where annual maximum temperatures are projected to increase by more than 4°C (Thorne et al., 2016). Such increasing temperature projections are anticipated to have important implications for evaporative demand and soil drying, especially in such arid grassland ecosystems of Southern California.

We used the SMBM model to explore the possible effects of such variations in P and PET on soil moisture and grassland vegetation in a simple parsimonious way, based on projections of shifting precipitation variability and evaporative demand (Berg & Hall, 2015; Pierce et al., 2018). In these explorations of specific types of climate change, we used monthly input data and did not alter other key parameters, such as soil properties and vegetation cover. The approach of only altering P or PET forcing of the SMBM allowed us to separately explore the influence of changes in precipitation and evaporative demand to moisture and plant water availability, under scenarios of more intense drought. The period 2012-01-01 to 2018-12-31 was used as a reference climate, and the experimental climate scenarios are represented as a deviation from it as follows:

Scenario A) Simulates the effects of a truncated rainy season (November – February) that reflects a loss of spring rains. This scenario represents an extreme decline in annual precipitation totals (average ~30% loss of annual P), the loss of precipitation in the shoulder seasons and thus prolonged dry periods.

Scenario B) Simulates redistribution of lost spring rains from Scenario A into the truncated rainy season from November – February, thus increasing the precipitation intensity and frequency during the compressed rainy season, combined with an increase in dry season length. Projections of CMIP5 indicated an increase in the number of dry days combined with increased frequencies of heavy precipitation, overall increasing interannual precipitation variability over California (Berg & Hall, 2015).

Scenario C) Simulates the effects of extreme drought. It uses Scenario A's loss of spring rains, along with increased evaporative demand combined with a 25% reduction in winter rainfall totals. Annual evaporative demand was increased to represent an average 4°C increase in annual temperature, characterized by more warming in the dry season, which is based

Deleted: Simple Climate Change

Deleted: with an increased number of dry days and increased evaporative demand…

Deleted: The projected

Deleted: corroborated

Deleted: as well as vegetation growth

Deleted: extreme

Deleted: We developed three simplistic climate change scenarios based on regional climate change projections.

Deleted: prolonged dry season and a

Deleted: from

Deleted: .

Deleted: ,

Deleted: historic precipitation totals over a

Deleted: .

Deleted: by 10%, while precipitation frequency and intensity remain unaltered from

Deleted: historical baseline. This scenario

Deleted: consistent with a 4°C

loosely on projected changes in temperature for Southern California and much of the Southwest (Cook et al., 2015) under RCP 8.5.

We retained dynamic vegetation responses in our investigation of the climate scenarios. To replace historic NDVI values (which do not exist for potential future scenarios), we developed a heuristic relationship between NDVI and available precipitation (aP) as aP= P – ET_0, and we determined over what antecedent time period aP most strongly influences vegetation responses (1,2 or 3 months), based on correlation strength (Pearson's correlation). We used a power law fit that best explained NDVI variation based on aP (using R^2 and root-mean-square-error RMSE), considering the non-drought, moderate and extreme drought separately. We use this regression to create a synthetic NDVI input for our climate change simulations based on internally generated aP and to estimate k_c based on Equation 1.

Deleted: change

Deleted: In addition, we

Deleted: net

Deleted: netP

Deleted: PET)

Deleted: evaluated the

Deleted: over which netP

Deleted: to establish a final regression form and selected a correlation model

Deleted: , as a result of netP, considering drought and non-drought periods separately, and used coefficient of determination (R^2)

Deleted: to evaluate

Deleted: chosen

Deleted: The relationship was used in the climate change simulations …

Deleted: based on artificial netP

Deleted: , which was then used

Deleted: and drive the SMBM.

3. Results

3.1 Meteorology of the Drought

The 2012-2019 drought in Southern California was marked by several years of above average temperatures, high evaporative demand, and low precipitation. The seasonal differences during the March – October dry season between drought periods was +0.7°C between non drought and moderate drought, +1.9 between non drought and extreme drought and +1.3 between moderate and extreme drought at the coastal site, and +1.1, +1.9 and +0.8 for the inland site, respectively. Daily maximum temperatures during March – October were on average 6.2°C warmer at the inland site. Temperature differences were significantly different between all drought periods at both sites (**Figure 4a**; **Table S3**). Due to the moderating effects of cooler/moister oceanic air and coastal fog, relative humidity at the coastal site averaged at 81%, (**Figure 4b**). Inland, the relative humidity was lower, averaging 54% under non-drought conditions, and decreasing significantly during the extreme drought to an average of 48%. The more moderate temperatures and high relative humidity at the coastal site were also reflected

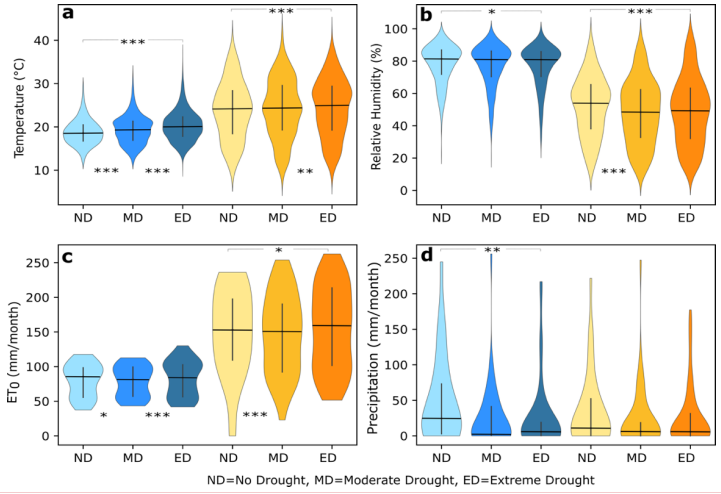

Figure 4: Violin plots showing historic climate variables. a) monthly mean daytime temperature, b) monthly mean relative humidity, c) monthly cumulative reference evapotranspiration (ET_0) and d) cumulative monthly precipitation during the non-drought, moderate and extreme drought for the coastal (blue hues) and inland (orange hues) site. The vertical black line indicates the interquartile range, the black horizontal line the median. Statistical differences are indicated as p< 0.05(*), p<0.01(**) and P<0.001(***).

Deleted: The

Deleted: *<object>*

Deleted: in Santa Barbara County.

Deleted: non-drought and

Deleted: 1

Deleted: 15°C at

Deleted: with daily

Deleted: the

Deleted: season being

Deleted: than at the coast.

Deleted: higher during the

Deleted: KS =0.15 at the coastal and 0.0098 at the inland site, $p=5.09^{e-5}$) (

Deleted: 77%, with no significant changes between non-drought and drought periods

Deleted: significantly

Deleted:

Deleted: (KS = 0.058, p=0.003), averaging 49

in a lower evaporative demand, resulting in ~50% lower annual PET compared to the inland site. Monthly PET averages at the coastal site were 265 mm/year and 515mm/year at the inland site during non-drought periods, with significant increases during the extreme drought period, especially at the inland site (**Figure 4c**). Historical annual precipitation over the 11-year period was on average 20% less at the inland site than at the coast, as the site lies in the rain shadow of the Santa Ynez mountain range. Precipitation averaged 147mm/year at the coastal site and 119 mm/year at the inland site during the non-drought period, with precipitation at the coastal site showing a significant shift towards lower monthly totals during drought periods (**Figure 4d**). The lowest October-September totals at both sites were recorded during the heart of the drought in 2014 with 170 mm/year at the coastal and 162 mm/year at the inland sites. A period of intense precipitation occurred from late 2016 – spring 2017, but

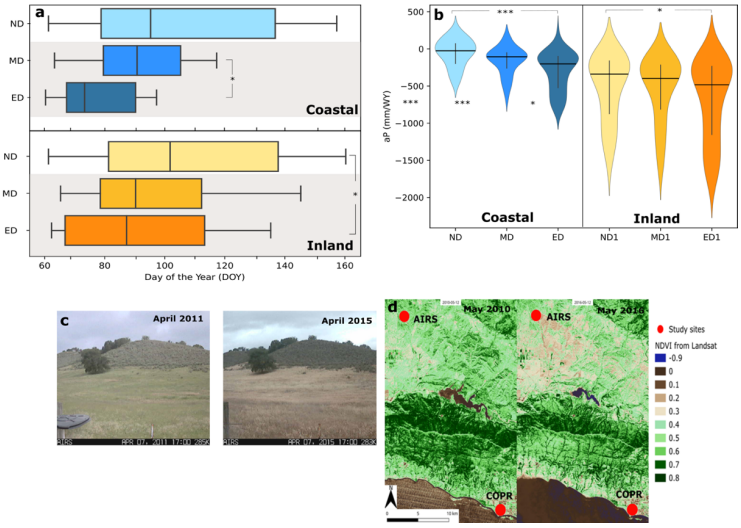

Figure 5: a) The onset of the dry season for the coastal (blue hues) and inland (orange hues) site, presented as day of the year (DOY). Vertical black lines indicate the median DOY, whiskers indicate the maximum and minimum DOY recorded. B) Violin plots of available P for a water year (October-September) for the non-drought, moderate and extreme drought period. Black horizontal lines indicate median aP and vertical lines the interquartile range. C) Webcam images of the inland site during non-drought (April 2011) and extreme drought (April 2015) highlight the early onset and decline of greenness at the height of the drought. d) Decline in greenness throughout the Santa Barbara county seen through NDVI images. Statistical significance is indicated as p<0.001 (***) and p<0.05(*)

Deleted: (**Figure 4c**).
Formatted: Font: Italic
Deleted: 87
Deleted: month
Deleted: 152 mm/month
Deleted: over the entire study period,
Deleted: (KS = 0.091, p=5.11^{e-5} coastal, KS= 0.093, p= 5.10^{e-5}
Deleted: site (**Figure 4d**). however there was no statistical significance in annual rainfall totals between non-drought and drought. High winter rains (382 mm/yr inland and 488 mm/yr coastal)…
Deleted: in

the area remained in a state of severe drought until early 2019. A single dry year in 2018 temporarily increased the drought stress on the region again, before a very wet rainy season in 2019 finally relieved the pressure on ecosystems and water resources in Santa Barbara County locations and the entire state (**Figure 2b**). Most notably was the emergence of a shift in the onset of the dry season, after which no more precipitation was recorded for three consecutive months or more, until the start of the rainy season again in the fall (**Figure 5a**). At the coastal site, we see that the shift of the onset of the dry season is most significant between non-drought and extreme drought, with a shift from DOY 95 to 73, which translates to a temporal shift roughly from early April to mid-March, whereas at the inland site, the shift was already noticeable, with the DOY shifting from 103 (non-drought) to 90 (moderate drought) to 87 (extreme drought). This shift in early dry season onset from mid-April to late March triggered visible vegetation browning during the extreme drought by late March/early April at the inland site, as opposed to a more gradual browning between May and June in the years preceding the drought (**Figure 5c,5d**). The increased evaporative demand and reduced precipitation during the drought also resulted in significant changes to available P during drought periods, implying limited water availability for infiltration and soil moisture, especially inland (**Figure 5b**).

Deleted:

Deleted: ¶
While there

Deleted: no significant difference in

Deleted: amount of total precipitation, there was

Deleted: or the (spring) day of the calendar year

Deleted: . During the drought, the dry season began at least one month earlier than during the non-drought period

Deleted: inland

Deleted: shifted

Deleted: a median

Deleted: 130

Deleted: 117

Deleted: mid-May to mid to late April. At the coastal site, the median DOY shifted from 151 to 109 during the drought, i.e. from late May to

Deleted: .

Deleted: Furthermore,

Deleted: a significantly lower netP (KS = 0.351, p = 0.00075 coastal, KS=0.253, p = 0.033 inland),

Deleted: further

Deleted: .

3.2 Soil Moisture and Plant Responses to Drought

765 The drought was expressed differently in the soil moisture at each site. Soil moisture observations showed increased drying of soils during drought periods at both sites, compared to the non-drought period, reaching extremely low moisture levels in 2013 and 2014 (daily saturation fell below 5% inland). Similar low soil moisture occurred at both sites in 2008, a particularly dry year for the SB region (**Figure 2b**). At both sites, monthly average saturation was significantly different between the non-drought and drought periods at both sites, with significantly lower levels during the drought at both sites (**Figure 6a**). Average 770 saturation was similar at both sites during the non-drought period (40%) but decreased to an average of 30% at the coastal site and 23% at the inland site during the extreme drought. At both sites average monthly NDVI during the non-drought period was significantly higher than during the drought periods (**Figure 6b**). Monthly NDVI values over selected non-drought and drought years illustrate the strong seasonality of annual grass cover in the region, with a marked green-up period after the winter rains, followed by a decline into brown conditions over the dry season (**Figure 6d,e**). In particular, there was a rapid

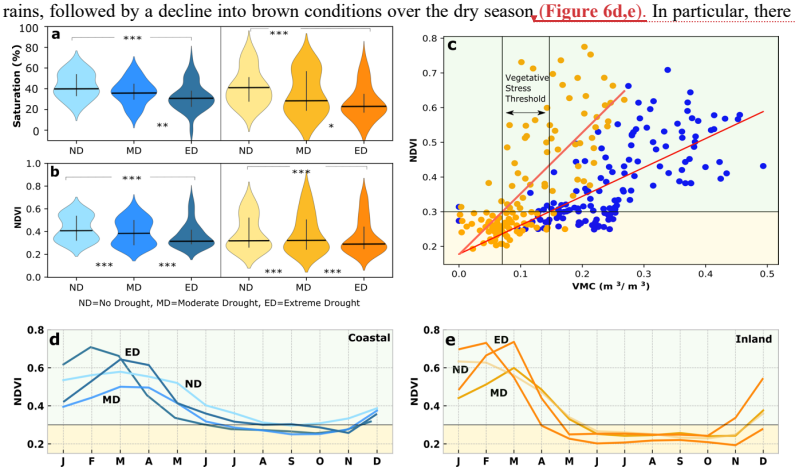

Figure 6: a) Monthly average saturation of soil moisture and b) daily mid-month NDVI during non-drought, moderate and extreme drought periods at the coastal (blue) and inland (orange) site. Medians are c) ch nd ues

Deleted: the

Deleted: degree of

Deleted: (**Figure 6a**).

Deleted: the median degree of

Deleted: KS=0.12, p=5.09^{e-5}

Deleted: , KS=0.224, p=5.09^{e-5}

Deleted:).¶
<object>

Deleted: reflect

Deleted: . Although the median NDVI values were not significantly different between non-drought and drought periods at either site (KS=0.14, p=0.54 coastal, KS=12, p=0.65 inland), there was an an increased variability between green up and vegetation die-off during drought.

increase of greenness during the extreme drought, following the winter rains in 2015 and 2016, and the subsequent unusually rapid and early decline of greenness in spring. Surprisingly, NDVI reached maximum values at the height of the drought in 2015 that were nearly double the non-drought averages (0.70 and 0.77 coastal and inland, respectively). It is notable that the NDVI peak values during drought were higher than those for the non-drought period at both sites, but very short-lived, as NDVI declines rapidly back to low values, in contrast to the shoulder of greenness and slower decline of NDVI that occurred in most non-drought years. During the extreme drought, NDVI dropped rapidly below 0.3 in April at the inland site, which was also visible in webcam images and spatial NDVI imagery over the region (**Figures 5c;6e**). These differences in the seasonal variation of NDVI suggest a strategy of rapid grass green up after winter rains, accelerated by mild winter temperatures during the drought, and especially during the exceptionally warm winter in 2014-2015. The growth of additional vegetation under these conditions likely led to the observed rapid decline in moisture during spring, as vegetation quickly depleted any excess moisture, and subsequently experienced increased browning and senescence due to the early onset of the dry season (**Figure 5a**). Correlation between NDVI and soil moisture of the concurrent month over our study period was strongly positive and statistically significant for both sites (R^2 = 0.68 coastal and inland, $p < 0.001$), a relationship that was used to establish a heuristic vegetation stress threshold at VMC = 0.15 m^3/m^3 for the coastal and VMC = 0.07 m^3/m^3 for the inland site. We associated these thresholds with very low rates of photosynthetic activity, based on an NDVI threshold of 0.3 (**Figure 6c**). Correlation between NDVI and aP over previous months revealed a three-month lag in aP and NDVI at the coastal site (R^2=0.82), and a two-month lag at the inland site (R^2=0.74). In order to develop a predictor (leading indicator) of vegetation response to aP, we fitted a linear regression models as follows:

$$NDVI_i = a * aP_m + b \qquad (4)$$

where $NDVI_i$ denotes an estimated monthly NDVI, aP_m is the amount of aP accumulated over a number of months m, and a and b are regression coefficients. A threshold of maximum NDVI was applied to both sites (0.75 coastal and 0.7 inland) during the regression analysis to account for the fact that NDVI saturates beyond a maximum amount of available water.

3.3. Soil Moisture Water Balance Model Performance

Given the simple structure of the SMBM, we were encouraged that the best models at each site were effective at capturing and predicting the timing and magnitude of interactions between P, PET, and soil moisture (**Figure 7a-b**). Kernel density estimates (KDE) for observed and simulated soil moisture distributions were statistically similar (**Figure 7c**; KS=0.12 and p=0.24 coastal and KS=0.12 and p=0.49 inland) and simulated and modelled soil moisture showed good correlation (R^2=0.84 coastal and R^2=0.84 inland). However, we note that the best-fit, simulated soil moisture at both sites may over- or under-estimate observed

Deleted: post… following the winter rains in 2015 and 2016, followed by an…nd the subsequent unusually rapid and early decline of greenness in spring (**Figures 6c;6d**)…. Surprisingly, NDVI reached maximum values in 2015 …t the height of the drought in 2015 that were nearly double the non-drought averages (0.70 and 0.77 coastal and inland, respectively). It is notable that the drought NDVI peak values are…uring drought were higher than those for the non-drought period at both sites, but they were …ery short-lived.…as NDVI dropped steeply…eclines rapidly back to low values, in contrast to the shoulder of greenness and slower decline of NDVI that occurred in most non-drought years (**Figure 6c;6d**). ¶ . During the extreme drought, NDVI dropped rapidly below 0.3 in April at the inland site, supporting the result seen in the…hich was also visible browning through …n webcam images and spatial NDVI imagery over the region (**Figures 5c;6c;6d…e**). These differences in the seasonal variation of NDVI suggest an aggressive… strategy of rapid grass green up after winter rains, accelerated by mild winter temperatures during the drought,…and especially during the exceptionally warm winter in 2014-2015. The growth of additional vegetation under these conditions likely led to the observed rapid decline in moisture during spring, as vegetation quickly depleted any excess moisture, and subsequently the…xperienced increased browning and senescence due to the early onset of the dry season. Pearson correlation…(**Figure 5a**). Correlation between NDVI and moisture of the concurrent month over our study period was strongly positive and statistically significant for both sites (R^2 = 0.68 coastal and inland, $p < 0.001$). The correlation between the two variables…, a relationship that was used to establish an… heuristic vegetation stress threshold at VMC = 0.17…5 m^3/m^3 for the coastal and VMC = 0.07 m^3/m^3 for the inland site, which we… We associated these thresholds with very low rates of photosynthetic activity, based on an NDVI threshold of 0.3 (**Figure 6e**). ... [8]

Deleted: Pearson correlation between NDVI and netP revealed a three-month lag in netP and NDVI at the coastal site (R^2=0.82), while at the inland site it was a two-month lag (R^2=0.74). In order to develop a predictor (leading indicator) of vegetation response to netP, we fitted regression models as follows: ¶ ... [9]

Deleted: predicted…n estimated monthly NDVI, $netP_m$…P_m is an…he amount of netP…P accumulated over a number of months m, and a and b are regression coefficients. The results of regression coefficients and correlation are shown in **Figure** ... [10]

Formatted: Font: Not Bold

Deleted: for each site…nland) during the drought and non-drought periods ... [11]

Formatted: Font: Bold

Deleted: ¶ ¶

Deleted: **8a…a-b**). Kernel density estimates (KDE) for observed and simulated soil moisture distributions were also …tatistically similar (**Figure 8c…c**; KS=0.086…2 and p=0.68…4 coastal and KS=0.14…2 and p=0.18…9 inland at p> … and simulated and modelled soil moisture showed good correlation (R^2=0.01). ... [12]

VMC at particular points in the time series. Notably, the best model from the Monte Carlo simulations at the inland site was not able to capture the extreme dryness in 2013 and 2014. The SMBM assumes plant wilting point as the lowest level of soil moisture. However, in reality soil moisture may decline below wilting point during extremely dry periods through shallow soil evaporation. In such conditions, senescent or even dead plants can also act as a medium for the transference of water long after wilting has occurred, potentially compounding the effects of soil drying by evaporation (Briggs and Shantz, 1912). Nash Sutcliffe Efficiency (NSE) coefficients showed good predictive abilities by the model (**Figure 7a, b**).

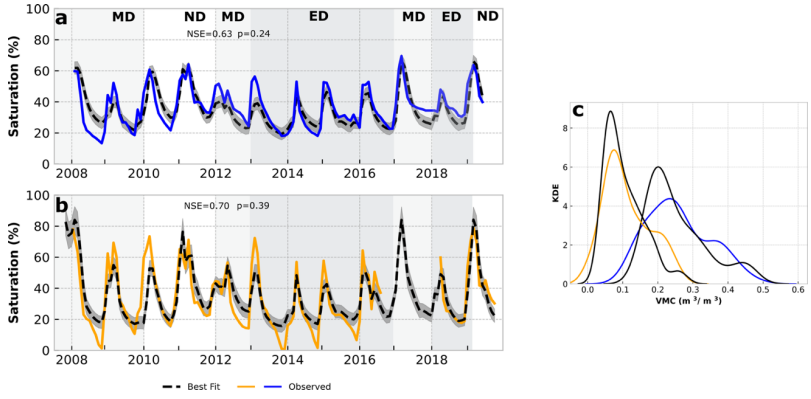

Figure 7: SMBM results for the a) coastal and b) inland site. Observed soil moisture is indicated in a solid line (blue-coastal, orange-inland), while simulated moisture is shown with a dashed black line. Grey shaded banding indicates ±1 Standard Deviation (SD) base on the output of 1000 Monte Carlo simulations. Grey vertical shading indicates non-drought (ND), moderate drought (MD) and extreme drought (ED) periods. c) KDE curves of the observed and simulated moisture for the best model fit confirm the functionality of the model. NSE and p values from Kolmogorov-Smirnov tests are indicated on a) and b), indicating statistical similarity between observed and simulated values.

3.3 Soil Moisture Responses to Plausible Future Drought Scenarios

Under historic drought conditions, simulations for both coastal and inland sites reveal a clear seasonal pattern of time below the vegetative stress threshold in the fall, prior to winter rainfall, which by extension represents the senescent periods typical for grasslands in Southern California (**Fig. 8a,b**). The differences in the extent of time below the threshold as well as the minimum saturation levels are visible between sites, and can be attributed to differences in soil water holding capacity and aridity. Inland, soil saturation is below the appointed threshold more than half (64%) the simulation time, compared to about 47% at the coastal site. Scenarios A and C noticeably shift soil moisture towards a drier baseline, leading to more extended

Deleted: is

Deleted: the

Deleted: .

Deleted: still

Deleted: *<object>***3.3 The response of soil moisture to plausible climate change scenarios**¶
Over the historic time frame studied here, modelled soil moisture at the coastal site was typically below the vegetative stress threshold, resulting in very low rates of photosynthetic activity (**Figure 6d**), prior to the onset of winter rains. Scenario A (truncated rainy season with precipitation occurring only between November to February) represents the loss of spring and early summer precipitation events, which results in a prolonged period of vegetative stress due to low soil moisture, beginning earlier in May. (**Figure 9b, coastal**). Scenario B (redistribution of the historical annual precipitation over a truncated rainy season between November to February), increases the intensity of rainfall events and thereby extends the duration of peak moisture levels in months of winter rainfall (broadened peaks in 2013 and 2015 and high associated VMC between January – April, **Figure 9c, coastal**). This result indicates lasting benefit from the simulated increased precipitation intensity, followed by several dry months of vegetative stress. Scenario C (increase of annual PET by 10%, reflecting ~4°C increase in annual temperature) drives a net reduction of soil moisture throughout the entire period and also an increase in the duration of the ***<object>***period with moisture levels below the vegetative stress threshold (**Figure 9d, coastal**). The increased climatic water deficit in this scenario could be conducive to a shifting baseline soil moisture towards drier conditions on average and drive coastal areas into more extreme and prolonged drought periods. Each scenario for the coastal site resulted in a strong statistical difference with the historic simulated moisture distribution (Scenario A: KS = 0.73, Scenario B: KS=0.63, Scenario C: KS=0.65 at p<0.001), underlining the soil moisture effects of extreme drought scenarios. ¶
Because of the warmer and more arid climate further inland, simulated changes in precipitation frequency and intensity further exacerbated the intense soil drying observed during the historical drought period (**Figure 9a, inland**). Scenario A created frequent occurrences where soil moisture would only reach peak levels briefly during and directly after the winter rains of particularly wet winter seasons (2013, 2015, 2016, 2017, **Figure 9b, inland**). In drier winters (2014, 2018), soil moisture only received minimal resupply and thus remained below the vegetative stress threshold. In Scenario B, the soil benefited from the simulated increased precipitation intensity during the winter. However, the early onset of the dry season and lack of spring precipitation pulses still resulted in simulated moisture levels dropping below the vegetative stress threshold for several months, creating an extended dry season **Figure 9c, inland**). Scenario C showed the effects of simulated increased evaporative demand on an already semi-arid landscape (**Figure 9d, inland**). The increase in evaporative demand would be sufficient to reduce simulated soil moisture to an increasingly dry stage from April onwards, with no moisture recharge despite precipitation later in the year because evaporative demand exceeds precipitation inputs. The simulated moisture scenarios for the inland site are statistically... [13]

periods of low saturation and the accumulation of an extreme soil moisture deficit extending over several years (**Fig. 8c, d, g, h**). Under Scenario C, for example, the time below the threshold would increase from the historical simulation by almost 50% at the coastal site and only 25% at the already dry inland site. This suggests that the previously buffered coastal locations would suffer disproportionally more from extended dry periods under extreme drought, as moisture reaches increasingly low levels previously unseen at this site. In contrast, the higher intensity P over the shortened rainy season in Scenario B actually reduces the amount of time below the stress threshold at the coastal site (by 2% or 76 days over the 8-yr simulation), and it only increases minimally by 2% at the coastal site (**Fig.8e, f**). In other words, redistributing the same annual P total into a briefer rainy season seems to mitigate the effects of no spring rains, and it also suggests a longer residence time of water in the

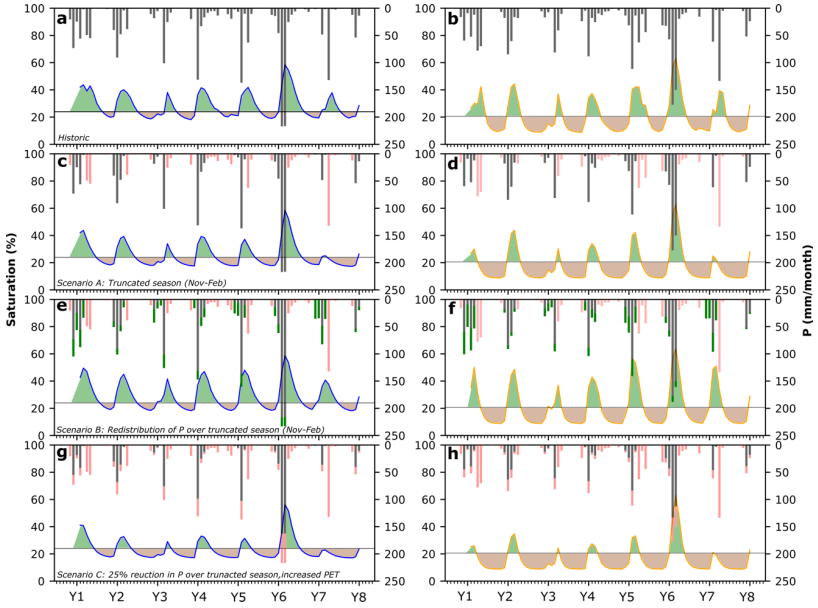

Figure 8: Simulations of soil moisture for the coastal and inland site. a) and b) show historic simulations. c) and d) Scenario A showing a truncated rainy season. Red bars indicate precipitation loss. e) and f) Scenario B showing a redistribution of annual P over the truncated season. Green bars indicate additional P, red bars indicate P loss. g) and h) Scenario C showing a truncated season with additional 25% loss of P and an increased PET demand equal to a +4°C increase in mean annual temperature. The horizontal ine indicates a vegetation stress threshold below which water becomes limiting to plants. Green shading indicates periods of greenness while brown shading highlights periods of senescence.

soil (especially at the coastal site) that persists into the summer. This would allow plants to access soil moisture storage even after precipitation has stopped and likely support normal plant growth over the season, without any extensive drying. Under Scenario B, the risk of extensive wildfires may also be less acute, as plants are not likely to suffer the level of intense and early senescence as would be seen in the other scenarios.

The loss of spring rains, with precipitation limited between November – February, artificially extends the dry period to a total of 8 months of the year (**Fig. 8c, d**), resulting in a loss of ~30% of the annual precipitation in Scenario A. Our simulations indicate that the loss of spring precipitation pulses in Scenario A seems to have a larger effect on the inland site. While the overall water input is reduced at both sites due to the shortening of the season, the amount of water removed as AET only reduces minimally (<5%) at the coastal site. However, at the inland site the loss of these events would result in the reduction of water used as AET by 10%, suggesting that the spring precipitation is a more important component of the water balance for this site (**Fig. 9b, e**). The low moisture holding capacity due to sandy soils and the more arid climate at the inland site, makes this site less resilient to the loss of spring precipitation at the time when plant development is about to start, and soil moisture is needed to support seed germination and biomass accumulation. Further analysis of the water balance suggests that the loss of spring rains seems to have only a minor effect on drainage (i.e. local potential groundwater recharge) at both sites, as drainage totals are only minimally reduced under Scenario A compared to historic values (**Fig 9c,f**). This suggests that precipitation events large enough to overcome antecedent soil moisture deficits and produce drainage only occur during the main winter months (Nov, Dec, Jan, Feb). Hence any precipitation lost by the shortening of the season would not have contributed towards groundwater recharge.

Scenario B represents an exploration of climate projections that increase the intensity of winter rains in Southern California with no change in total wetness, expressed as an increased number of large daily P events, which increases the monthly totals during the shortened season (**Fig. 8e,f**). At the coastal site, the redistribution of precipitation seems to have little effect on the percentage of P removed by AET, suggesting a tight coupling of AET to precipitation at this site. At the inland site, however, the fraction of precipitation removed as AET declines by ~10% compared to the historical simulation (**Fig. 9b,e**). It appears

that higher intensity rain events at the inland site may be large enough to promote deep infiltration and local drainage below the evaporation zone (e.g., in Y5), due to the low water holding capacity of the soils.

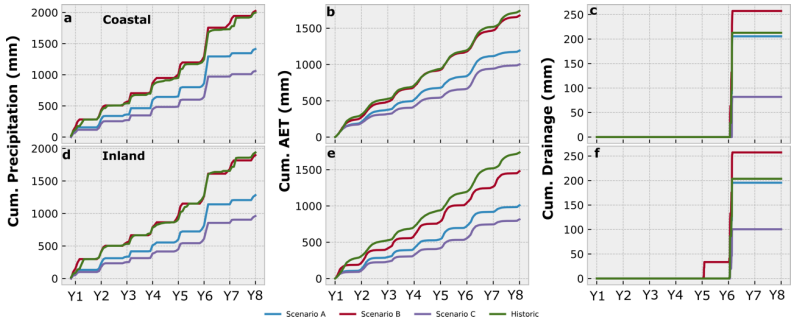

Figure 9: Cumulative water balance results for the coastal (top) and inland (bottom) site. a) and d) Cumulative precipitation shows the changes in available water between different scenarios. a) and d) The proportion of available water used as AET varies among scenarios and shows a tight coupling of AET and P at the coastal site. c) and f) Drainge only occurs after reaching certain thresholds of monhtly precipiation with the inland site benefitting from the added intensity in Scenario B, which resulted in extra drainge in Y5.

Rainfall event size and antecedent conditions together control drainage in our model, but our results indicate approximate rainfall thresholds that need to be overcome on daily and monthly timescales for drainage to occur. For example, a monthly total of >140 mm of precipitation at the inland site is the threshold above which drainage occurs. The events in Y6 both exceeded this threshold and produced considerable drainage for all simulations, with more than 50% of the incoming precipitation in those months becoming drainage. In contrast, the coastal site requires more precipitation to produce drainage with a monthly threshold >230 mm, suggesting that much more of the annual rainfall is recycled to the atmosphere. On a daily timescale, drainage occurence at the inland site corresponds to events of >20 mm/d, which produce an additional drainage peak in Y5, while the coastal site requires several days of rainfall between 20 – 55 mm/d to produce drainage. Overall, it is evident that the increased precipitation intensity would contribute towards increasing the overall amount of drainage at both sites (**Figure 9c,f**), with the added intensity increasing the potential for additional drainage and groundwater recharge at the inland site, despite the extended dry periods.

Deleted: smore to produce drainage withthreshold

In the extreme drought conditions of Scenario C, the effects of the increased precipitation loss and heightened PET affect several aspects of the water balance. The further reduction of precipitation over a shortened season has a major impact on soil

moisture with increasing low levels of saturation at both sites. As less water would be available overall at both sites, cumulative drainage is reduced >50% compared to the historical simulation (**Figure 9c,f**) and the loss of input precipitation by AET would be reduced at the inland site by up to 5%, due to less water being available to be used by plants. Interestingly, at the coastal site AET exceeds input precipitation by ~6% over the simulation period, reflecting an overall drying of these coastal soils under extreme drought.

4 Discussion

In light of the progression of climate change in semiarid environments such as Southern California, a better understanding of drought propagation and the climatic drivers of shifts in soil moisture and water availability to grassland vegetation (and correspondingly, to the health and functioning of grassland ecosystems), would enable anticipation of how soil moisture and grassland dynamics might respond to intensified moisture limitations under future scenarios of climate change across the region. The severity of the recent synoptic California drought and its effects on vegetation were most notably documented through upland forest canopy water stress and mortality (Asner et al., 2016; Fettig et al., 2019; Goulden & Bales, 2019), as well as through declining groundwater levels that heavily impacted agricultural production throughout the Central Valley (Thomas et al., 2017; Xiao et al., 2017). Similarly, the intensified moisture loss and accelerated ET also impacted lowland vegetation in Southern California, including differential species responses within chaparral and grassland ecosystems (Breshears et al., 2005; Gremer et al., 2015; Okin et al., 2018; Wilson et al., 2018). While the landscape in Southern California is dominated by vast stretches of brown grasslands during the dry season, the 2012-2019 drought hit Santa Barbara Country with considerable intensity and persistence, compared to the rest of the state (**Figure 2**), and propagated into multiple years of soil moisture deficits and early die-off of grasses **(Figures 4-6)**.

Our analysis revealed that winter/spring precipitation deficits, coupled with higher evaporative demand in Southern California, led to temporal shifts in the onset of the dry season, which in turn also led to increased soil drying in spring and summer. The loss of essential precipitation pulses in spring months generated large soil moisture deficits and induced a faster die-off (browning) of grasses, especially at the inland site. We explored this shift in dry season onset further by simulating soil moisture responses under an even shorter rainy season. Our findings suggest that arid sites such as our inland site with low water holding capacities, widespread over the region and more broadly over the Southwest and other Mediterranean climate systems, would become increasingly vulnerable to climate change that favors milder winter and hotter summer temperatures, and decreased precipitation in key months during spring. Sites with low moisture holding capacities due to sandy soils and more arid climate, seem less resilient to the loss of rain at the time when plant development is about to start and moisture is

Deleted:

Deleted: , it is essential to understand how lowland

Deleted: responded to the recent multi-year drought in Southern California. This

Deleted: predictions and/or

Deleted: Understanding the climatic drivers of shifts in soil moisture and water availability to vegetation (and correspondingly, to the health and functioning of grassland ecosystems), are fundamental for managing and ameliorating the negative impacts of climate change.

Deleted: in

Deleted: was so intense

Deleted: prolonged

Deleted: that it

Deleted: ,

Deleted:), and an overall drier landscape primed for fire. Previous studies have noted that increased greenness during spring exacerbated soil drying in the summer (Lian et al., 2020) and our study showed that the above average temperatures in combination with changes in the deliverance of winter precipitation led to an early and increased vegetation green up which resulted in accelerated soil drying in spring and unusually early senescent vegetation by April.

Deleted: . Our modeling analysis

Deleted: highlighted connections and feedbacks between climate and grassland vegetation in Southern California, which may be sensitive to climate change.

Deleted: vegetation communities

Deleted: are becoming increasingly vulnerable to climate change that favors milder winter temperatures and increased precipitation variability, thus increasing drought frequency and magnitude. In arid regions, the capacity of soils to store water becomes increasingly important as soil moisture can mitigate the impact of drought on grassland vegetation health (Gremer et al., 2015). The results from contrasting sites (coastal and inland) corroborate studies showing differential responses to the drought over short distances due to spatial variation in soil texture (Gremer et al., 2015; Liu et al., 2012; Okin et al., 2018) (**Figures 5;6**). Such differences in soils between our sites, despite similar vegetation, produced different responses to the driving climate. For example, the lower water holding capacity and higher evaporative demand of the inland site led to much earlier senescence, selectively priming it for large and destructive wildfires and likely bringing these ecosystems to their physiological limit. This result can be viewed alongside prior work in the Southwest suggesting that

needed for seed germination and plant groth. Interestingly, the potential for apparent local groundwater recharge seems to remain unaffected by the loss of spring rains, suggesting that drainage only occurs during the winter months and even under prolonged periods of drought there is potential for local groundwater recharge. Such changes to the seasonal delivery of precipitation would increase the soil moisture drought frequency and magnitude, leading to much earlier senescence of vegetation and widespread desertification of the landscape, while selectively priming the landscape for large and destructive wildfires, thus suggesting that already arid ecosystems might be brought to their physiological limit. These result can be viewed alongside prior work in the Southwest that suggested chapparal landscapes (Okin et al., 2018) and perennial (C_4) grasslands (Gremer et al., 2015) are increasingly prone to negative impacts from drought. Given how widespread the recent drought was in terms of spatial footprint and temporal length, more frequent occurrence of extreme drought conditions in the future could be devastating to perennial grasses and chapparal communities with larger consequences for entire grassland/shrubland ecosystems over a broad spatial extent (Gremer et al., 2015; Okin et al., 2018; Petrie et al., 2015).

With climate change projected to impact the temperate and precipitation regimes in California, and much of the Southwestern U.S., the frequency and magnitude of droughts and drought-like conditions are expected to increase (Bradford et al., 2020; Diffenbaugh et al., 2015). Under a more severe emission scenario of RCP 8.5, the frequency of extreme dry years is projected to almost triple with temperatures projected rise by up to 4°C throughout California (Pierce et al., 2018; Thorne et al., 2016). Precipitation projections remain uncertain (Pierce et al., 2018, Bradford et al., 2019), but given the degree of already existing aridity in the Southwest, even relatively modest changes to precipitation intensity and timing would create conditions much more conducive to prolonged drought periods. One climate scenario explored the combination of increased evaporative demand and decreased precipitation intensity and frequency, and the results highlighted the potential for multi-year soil moisture droughts to occur at even previously less affected coastal sites. Under such a conditions evaporative demand would exceed water availability, leaving coastal areas in a state of severe soil moisture deficit, thus putting a new strain on these ecologically sensitive areas and leave them potentially unsuitable as climate refugia and habitats for critical threatened and endangered species in the future.

Another key finding of the climate sumulations has revealed that the occurance of extreme events after prolonged periods of drought, as simulated in Scenarios A and B, would provide temporary relief to soil moisture, and most likely support considerable green up and production of biomass during that season. However, if climate conditions revert to extreme dryness and minimal precipitation input during the following year, the soil moisture deficit would increase again to a level unlikely to support the extensive growth from the previous season. Under these conditions the senescent vegetation would turn into easily

Deleted: With a broader perspective of responses to water limitations in vegetation communities across arid and semi-arid lands in the Southwest, our results underscore that climate change impacts may differ substantially over short distances, thus affecting large areas of annual grasses, perennial grasses, and chapparal vegetation in more arid environments beyond their ability to adapt to these shifts, potentially priming increasingly large areas for widespread wildfires and increase the risk of widespread desertification of the landscape.¶
Grassland habitats in arid and semiarid environments are especially sensitive to changes in evaporative demand, amount and timing of precipitation and soil moisture availability (Gremer et al., 2015; Liu et al., 2012; Munson, 2013; Peters and Yao, 2012). The 2012-2019 California drought exemplified many of the potential deleterious effects of climate on vegetation communities (a truncated rainy season, increased evaporative demand, and longer dry periods), which led to an early die-back of annual grasses. Given how widespread this last drought was in terms of spatial footprint and temporal length, the effects of such drought conditions

Deleted: If these sorts of drought occur in the future and if they intensify, it is expected to lead to dramatic shifts in soil moisture towards a drier baseline for extended periods. This outcome could potentially leave grassland species diversity and productivity severely compromised, due to increased susceptibility to encroachment of invasive species and expansion of shrublands, thus limiting native species regeneration (Bradford et al., 2020; Peters et al., 2010; Reynier et al., 2017). Earlier and longer dry seasons with increased temperatures and increased evaporative losses and soil drying also reduce surface evaporative cooling and increase the possibility of more intense summer heatwaves (Lian et al., 2020). We also might expect conditions more conducive to large and widespread wildfires due to greater and deeper drying of soils and vegetation, raising the impact of fire severity and extent to new unprecedented levels in an already fire-prone region (Westerling et al, 2006; 2007). The increasing intrusion of invasive annual grasses has been linked to an increase in lighter fuels, leading to conditions under which fires ar... [14]

Deleted: is

Deleted: and

Deleted: are

Deleted: to increase

Deleted: frequency would create conditions much more conducive to prolonged drought periods. The increased occurrence of extended dry periods would slow down the recovery from moisture deficit inherited from prior drought conditions, raising the potential for soil moisture deficits to accumulate to unprecedented levels (Diffenbaugh et al., 2015). Such changes to the climate system, partially ... [15]

Deleted: Similarly, the increased loss of moisture from elevated temperatures in semi-arid regions further inland could induce widespread desertification of the landscape, an increasingly altered species composition and abundance and chronic moisture deficits, thus negatively impacting grassland ecosystems over a broad spatial extent. …

ignitable fuel that, and coupled with the dried-out soils, would prime the landscape for extensive wildfires, thus potentially creating a severe chain reaction of extreme events as previously seen during the Montecito fires and mudslides.

5 Conclusion

The 2012-2019 drought in California had profound impacts on soil moisture and vegetation. Employing long-term monitoring data, we delineated the differential responses of soil moisture and vegetation dynamics of grassland ecosystems to this unprecedented, multi-year drought in Southern California. A temporal shift of dry season onset led to early senescence and browning of vegetation and rendered soil moisture resources prematurely exhausted, and the landscape primed for easily ignitable and widespread wildfires. During the drought, temporal patterns of vegetation productivity changed, including increased greenness attributed to mild winter temperatures after prolonged dry periods. However, this new vegetation growth quickly reached a state of senescence due to the early onset of the dry season, exacerbating the soil moisture deficit.

Through a simple, parsimonious soil moisture water balance model, we further explored the moisture dynamics and water balance in terms of soil moisture for grasslands under different conditions that represent possible simplistic climate change scenarios. We linked soil moisture and vegetation response through NDVI and explored the effects of various changes to precipitation and evaporative demand. The results suggest that such changes could have unprecedented effects on soil moisture and water availability to grassland ecosystems, leading to rapid die-back and prolonged desiccation of the landscape. Our result highlighted the differential responses of moisture and vegetation over a small geographical area. In future, more extreme and prolonged droughts, characterized by a shorter rainy season, higher evaporative demand, and/or protracted dry periods, will likely lead to increased soil moisture deficits at sites with low water holding capacities, as moisture levels are likely to drop to a level of elevated vegetative stress for much of the year. The combination of such climate induced changes, loss of precipitation pulses in spring and summer, a continuing shift of early dry season onset and increased evaporative demand, are likely contributors to affect grassland ecosystems in future and drive even previously less affected coastal areas into more severe droughts, as well as induce widespread desertification of the landscape in semi-arid environments. A shift to a drier moisture baseline of soils and vegetation could potentially have deleterious effects on species diversity, increase the risk of shrub encroachment and invasive species and leave the region overall more prone to destructive and widespread wildfires.

Deleted: Through

Deleted: the

Deleted: ignited

Deleted: there were changes in the

Deleted: dried out

Deleted: future

Deleted: climate change scenarios. The results suggest that

Deleted: an

Deleted: The

Deleted: buffered

Deleted: more

References

Abatzoglou, J. T. and Kolden, C. A.: Climate change in Western US deserts: Potential for increased wildfire and invasive annual grasses, Rangel. Ecol. Manag., 64(5), 471–478, doi:10.2111/REM-D-09-00151.1, 2011.

Abatzoglou, J. T. and Williams, A. P.: Impact of anthropogenic climate change on wildfire across western US forests, Proc. Natl. Acad. Sci. U. S. A., 113(42), 11770–11775, doi:10.1073/pnas.1607171113, 2016.

Aghakouchak, A., Ragno, E. and Love, C.: Projected Changes in Californias Precipitation Intensity-Duration-Frequency Curves, in California's Fourth Climate Change Assessment, p. 32, California Energy Commission., 2018.

Allen, R. G., Pereira, L. S., Raes, D. and Smith, M.: FAO Irrigation and Drainage Paper No. 56, Crop evapotranspiration (Guidelines for computing crop water requirements). [online] Available from: http://www.kimberly.uidaho.edu/water/fao56/, 1998.

Asner, G. P., Brodrick, P. G., Anderson, C. B., Vaughn, N., Knapp, D. E. and Martin, R. E.: Progressive forest canopy water loss during the 2012-2015 California drought, Proc. Natl. Acad. Sci. U. S. A., 113(2), E249–E255, doi:10.1073/pnas.1523397113, 2016.

Ault, T. R., Mankin, J. S., Cook, B. I. and Smerdon, J. E.: Relative impacts of mitigation, temperature, and precipitation on 21st-century megadrought risk in the American Southwest, Sci. Adv., 2(10), 1–9, doi:10.1126/sciadv.1600873, 2016.

Berg, N. and Hall, A.: Increased interannual precipitation extremes over California under climate change, J. Clim., 28(16), 6324–6334, doi:10.1175/JCLI-D-14-00624.1, 2015a.

Berg, N. and Hall, A.: Interannual Precipitation Extremes over California Under Climate Change, J. Clim., 53(9), 287, doi:10.1017/CBO9781107415324.004, 2015b.

Berg, N. and Hall, A.: Anthropogenic warming impacts on California snowpack during drought, Geophys. Res. Lett., 44(5), 2511–2518, doi:10.1002/2016GL072104, 2017.

Bradford, J. B., Schlaepfer, D. R., Lauenroth, W. K. and Palmquist, K. A.: Robust ecological drought projections for drylands in the 21st century, Glob. Chang. Biol., (December 2019), 3906–3919, doi:10.1111/gcb.15075, 2020.

Breshears, D. D., Cobb, N. S., Rich, P. M., Price, K. P., Allen, C. D., Balice, R. G., Romme, W. H., Kastens, J. H., Floyd, M. L., Belnap, J., Anderson, J. J., Myers, O. B. and Meyer, C. W.: Regional vegetation die-off in response to global-change-type drought, Proc. Natl. Acad. Sci., 102(42), 15144–15148, doi:10.1073/pnas.0505734102, 2005.

Briggs, L. J. and Shantz, H. L.: The Wilting Coefficient and Its Indirect Determination, Bot. Gaz., 53(1), 20–37, 1912.

Caylor, K. K., D'Odorico, P. and Rodriguez-Iturbe, I.: On the ecohydrology of structurally heterogeneous semiarid landscapes, Water Resour. Res., 42(7), 1–13, doi:10.1029/2005WR004683, 2006.

Caylor, K. K., Scanlon, T. M. and Rodriguez-Iturbe, I.: Ecohydrological optimization of pattern and processes in

Formatted: Font colour: Auto, English (UK)
Deleted: Rangeland Ecology and Management,
Formatted: Font colour: Auto, English (UK)
Deleted: Proceedings of the National Academy of Sciences of the United States of America,
Formatted: Font colour: Auto, English (UK)
Deleted: Proceedings of the National Academy of Sciences of the United States of America,
Formatted: Font colour: Auto, German (Austria)
Formatted: Font colour: Auto, English (UK)
Deleted: Science Advances,
Formatted: Font colour: Auto, English (UK)
Deleted: Berg, A. and Sheffield, J.: Climate Change and Drought: the Soil Moisture Perspective, Current Climate Change Reports, 4(2), 180–191, doi:10.1007/s40641-018-0095-0, 2018.¶
Formatted: Font colour: Auto, English (UK)
Deleted: Journal of Climate,
Formatted: Font colour: Auto, English (UK)
Deleted: Journal of Climate,
Formatted: Font colour: Auto, English (UK)
Deleted: Geophysical Research Letters,
Formatted: Font colour: Auto, English (UK)
Deleted: Bonan, G. B.: Land surface model (LSM version 1.0) for ecological, hydrological, and atmospheric studies: Technical description and user's guide. Technical note., 1996.¶
Formatted: Font colour: Auto, English (UK)
Deleted: Global Change Biology,
Formatted: Font colour: Auto, English (UK)
Deleted: Proceedings of the National Academy of Sciences,
Formatted: Font colour: Auto, English (UK)
Deleted: Botanical Gazette,
Formatted: Font colour: Auto, English (UK)
Deleted: Resources Research,
Formatted: Font colour: Auto, English (UK)

water-limited ecosystems: A trade-off-based hypothesis, Water Resour. Res., 45(8), 1–15, doi:10.1029/2008WR007230, 2009.

Coates, A. R., Dennison, P. E., Roberts, D. A. and Roth, K. L.: Monitoring the impacts of severe drought on southern California Chaparral species using hyperspectral and thermal infrared imagery, Remote Sens., 7(11), 14276–14291, doi:10.3390/rs71114276, 2015.

Cook, B. I., Ault, T. R. and Smerdon, J. E.: Unprecedented 21st century drought risks in the American south west and central plains, Sci. Adv., 1 e1400081(February), 1–8, 2015.

Cuthbert, M. O., MacKay, R. and Nimmo, J. R.: Linking soil moisture balance and source-responsive models to estimate diffuse and preferential components of groundwater recharge, Hydrol. Earth Syst. Sci., 17(3), 1003–1019, doi:10.5194/hess-17-1003-2013, 2013.

Cuthbert, M. O., Taylor, R. G., Favreau, G., Todd, M. C., Shamsudduha, M., Villholth, K. G., MacDonald, A. M., Scanlon, B. R., Kotchoni, D. O. V., Vouillamoz, J. M., Lawson, F. M. A., Adjomayi, P. A., Kashaigili, J., Seddon, D., Sorensen, J. P. R., Ebrahim, G. Y., Owor, M., Nyenje, P. M., Nazoumou, Y., Goni, I., Ousmane, B. I., Sibanda, T., Ascott, M. J., Macdonald, D. M. J., Agyekum, W., Koussoubé, Y., Wanke, H., Kim, H., Wada, Y., Lo, M. H., Oki, T. and Kukuric, N.: Observed controls on resilience of groundwater to climate variability in sub-Saharan Africa, Nature, 572(7768), 230–234, doi:10.1038/s41586-019-1441-7, 2019.

D'Odorico, P., Caylor, K., Okin, G. S. and Scanlon, T. M.: On soil moisture-vegetation feedbacks and their possible effects on the dynamics of dryland ecosystems, J. Geophys. Res. Biogeosciences, 112(4), 1–10, doi:10.1029/2006JG000379, 2007.

Diffenbaugh, N. S., Swain, D. L. and Touma, D.: Anthropogenic warming has increased drought risk in California, Proc. Natl. Acad. Sci., 112(13), 3931–3936, doi:10.1073/pnas.1422385112, 2015.

Dong, C., MacDonald, G. M., Willis, K., Gillespie, T. W., Okin, G. S. and Williams, A. P.: Vegetation Responses to 2012–2016 Drought in Northern and Southern California, Geophys. Res. Lett., 3810–3821, doi:10.1029/2019GL082137, 2019.

Donovan, V. M., Twidwell, D., Uden, D. R., Tadesse, T., Wardlow, B. D., Bielski, C. H., Jones, M. O., Allred, B. W., Naugle, D. E. and Allen, C. R.: Resilience to large, 'catastrophic' wildfires in North America's grassland biome, Earth's Futur., doi:10.1029/2020ef001487, 2020.

Evans, C. M., Dritschel, D. G. and Singer, M. B.: Modeling Subsurface Hydrology in Floodplains, Water Resour. Res., 54(3), 1428–1459, doi:10.1002/2017WR020827, 2018.

Fettig, C. J., Mortenson, L. A., Bulaon, B. M. and Foulk, P. B.: Tree mortality following drought in the central and southern Sierra Nevada, California, U.S., For. Ecol. Manage., 432(September 2018), 164–178, doi:10.1016/j.foreco.2018.09.006, 2019.

Gillespie, T. W., Ostermann-kelm, S., Dong, C., Willis, K. S., Okin, G. S. and Macdonald, G. M.: Monitoring changes of NDVI in protected areas of southern California, Ecol. Indic., 88(June 2017), 485–494, doi:10.1016/j.ecolind.2018.01.031, 2018.

Deleted: Resources Research,
Formatted: Font colour: Auto, English (UK)
Deleted: Sensing,
Formatted: Font colour: Auto, English (UK)
Deleted: Science Advances,
Formatted: Font colour: Auto, English (UK)
Deleted: Hydrology and
Formatted: Font colour: Auto, English (UK)
Deleted: System Sciences,
Formatted: Font colour: Auto, English (UK)
Deleted: Journal of Geophysical Research:
Formatted: Font colour: Auto, English (UK)
Deleted: Davin, E. L., Maisonnave, E. and Seneviratne, S. I.: Is land surface processes representation a possible weak link in current Regional Climate Models?, Environmental Research Letters, 11(7), doi:10.1088/1748-9326/11/7/074027, 2016.¶
Formatted: Font colour: Auto, English (UK)
Deleted: Proceedings of the National Academy of Sciences,
Formatted: Font colour: Auto, English (UK)
Deleted: Geophysical Research Letters,
Formatted: Font colour: Auto, English (UK)
Deleted: Future,
Formatted: Font colour: Auto, English (UK)
Deleted: Resources Research,
Formatted: Font colour: Auto, English (UK)
Deleted: Farrar, T. J., Nicholson, S. E. and Lare, A. R.: The influence of soil type on the relationships between NDVI, rainfall, and soil moisture in semiarid Botswana. I. NDVI response to rainfall, Remote Sensing of Environment, 50(2), 107–120, doi:10.1016/0034-4257(94)90038-8, 1994.¶
Formatted: Font colour: Auto, English (UK)
Deleted: Forest Ecology and Management,
Formatted: Font colour: Auto, English (UK)
Deleted: Ecological Indicators,
Formatted: Font colour: Auto, English (UK)

Glenn, E. P., Neale, C. M. U., Hunsaker, D. J. and Nagler, P. L.: Vegetation index-based crop coefficients to estimate evapotranspiration by remote sensing in agricultural and natural ecosystems, Hydrol. Process., 25(26), 4050–4062, doi:10.1002/hyp.8392, 2011.

Goulden, M. L. and Bales, R. C.: California forest die-off linked to multi-year deep soil drying in 2012–2015 drought, Nat. Geosci., 12(August), doi:10.1038/s41561-019-0388-5, 2019.

Gremer, J. R., Bradford, J. B., Munson, S. M. and Duniway, M. C.: Desert grassland responses to climate and soil moisture suggest divergent vulnerabilities across the southwestern United States, Glob. Chang. Biol., 21(11), 4049–4062, doi:10.1111/gcb.13043, 2015.

Gu, Y., Hunt, E., Wardlow, B., Basara, J. B., Brown, J. F. and Verdin, J. P.: Evaluation of MODIS NDVI and NDWI for vegetation drought monitoring using Oklahoma Mesonet soil moisture data, Geophys. Res. Lett., 35(22), 1–5, doi:10.1029/2008GL035772, 2008.

Hunsaker, D. J., Pinter, P. J. and Kimball, B. A.: Wheat basal crop coefficients determined by normalized difference vegetation index, Irrig. Sci., (24), 1–14, doi:10.1007/s00271-005-0001-0, 2005.

Keeley, J. E. and Syphard, A. D.: Climate change and future fire regimes: Examples from California, Geosci., 6(3), 1–14, doi:10.3390/geosciences6030037, 2016.

Lian, X., Piao, S., Li, L. Z. X., Li, Y., Huntingford, C., Ciais, P., Cescatti, A., Janssens, I. A., Peñuelas, J., Buermann, W., Chen, A., Li, X., Myneni, R. B., Wang, X., Wang, Y., Yang, Y., Zeng, Z., Zhang, Y. and McVicar, T. R.: Summer soil drying exacerbated by earlier spring greening of northern vegetation, Sci. Adv., 6(1), 1–12, doi:10.1126/sciadv.aax0255, 2020.

Liu, S., Roberts, D. A., Chadwick, O. A. and Still, C. J.: Spectral responses to plant available soil moisture in a Californian Grassland, Jnt. J. Appl. Earth Obs. Geoinf., 19(1), 31–44, doi:10.1016/j.jag.2012.04.008, 2012.

Ludwig, J. A., Wilcox, B. P., Breshears, D. D., Tongway, D. J. and Imeson, A. C.: Vegetation patches and runoff-erosion as interacting ecohydrological processes in semiarid landscapes, Ecology, 86(2), 288–297, doi:10.1890/03-0569, 2005.

McDowell, N., Pockman, W. T., Allen, C. D., Breshears, D. D., Cobb, N., Kolb, T., Plaut, J., Sperry, J., West, A., Williams, D. G. and Yepez, E. A.: Mechanisms of plant survival and mortality during drought: Why do some plants survive while others succumb to drought?, New Phytol., 178(4), 719–739, doi:10.1111/j.1469-8137.2008.02436.x, 2008.

Michaelides, K., Lister, D., Wainwright, J. and Parsons, A. J.: Vegetation controls on small-scale runoff and erosion dynamics in a degrading dryland environment, Hydrol. Process., (23), 1617–1630, 2009.

Munson, S. M.: Plant responses, climate pivot points, and trade-offs in water-limited ecosystems, Ecosphere, 4(9), 1–15, doi:10.1890/ES13-00132.1, 2013.

Nagler, P. L., Cleverly, J., Glenn, E., Lampkin, D., Huete, A. and Wan, Z.: Predicting riparian evapotranspiration from MODIS vegetation indices and meteorological data, Remote Sens. Environ., 94(1), 17–30, doi:10.1016/j.rse.2004.08.009, 2005.

Formatted: Font colour: Auto, English (UK)

Deleted: Nature Geoscience,

Formatted: Font colour: Auto, English (UK)

Deleted: Global Change Biology,

Formatted: Font colour: Auto, English (UK)

Deleted: Geophysical Research Letters,

Formatted: Font colour: Auto, English (UK)

Deleted: Irrigation Science,

Formatted: Font colour: Auto, English (UK)

Deleted: Kamble, B., Irmak, A. and Hubbard, K.: Estimating Crop Coefficients Using Remote Sensing-Based Vegetation Index, Remote Sensing, (5), 1588–1602, doi:10.3390/rs5041588, 2013.¶

Formatted: Font colour: Auto, English (UK)

Deleted: Geosciences (Switzerland),

Formatted: Font colour: Auto, English (UK)

Deleted: Science Advances,

Formatted: Font colour: Auto, English (UK)

Deleted: International Journal of Applied Earth Observation and Geoinformation,

Formatted: Font colour: Auto, English (UK)

Deleted: Phytologist,

Formatted: Font colour: Auto, English (UK)

Deleted: Hydrological Processes,

Formatted: Font colour: Auto, English (UK)

NDMC: United States Drought Monitor, United States Drought Monit, [online] Available from: https://droughtmonitor.unl.edu/, 2020.

Oakley, N. S., Cannon, F., Munroe, R., Lancaster, J. T., Gomberg, D. and Martin Ralph, F.: Brief communication: Meteorological and climatological conditions associated with the 9 January 2018 post-fire debris flows in Montecito and Carpinteria, California, USA, Nat. Hazards Earth Syst. Sci., 18(11), 3037–3043, doi:10.5194/nhess-18-3037-2018, 2018.

Okin, G. S., Dong, C., Willis, K. S., Gillespie, T. W. and MacDonald, G. M.: The Impact of Drought on Native Southern California Vegetation: Remote Sensing Analysis Using MODIS-Derived Time Series, J. Geophys. Res. Biogeosciences, 123(6), 1927–1939, doi:10.1029/2018JG004485, 2018.

Peters, D. P. C. and Yao, J.: Long-term experimental loss of foundation species: consequences for dynamics at ecotones across heterogeneous landscapes, Ecosphere, 3(3), art27, doi:10.1890/es11-00273.1, 2012.

Peters, D. P. C., Herrick, J. E., Monger, H. C. and Huang, H.: Soil-vegetation-climate interactions in arid landscapes: Effects of the North American monsoon on grass recruitment, J. Arid Environ., 74(5), 618–623, doi:10.1016/j.jaridenv.2009.09.015, 2010.

Petrie, M. D., Collins, S. L. and Litvak, M. E.: The ecological role of small rainfall events in a desert grassland, Ecohydrology, 8(8), 1614–1622, doi:10.1002/eco.1614, 2015.

Pierce, D. W., Kalansky, J. F. and Cayan, D. R.: Climate, Drought, and Sea Level Rise Scenarios for the Fourth California Climate Assessment, in California's Fourth Climate Change Assessment, California Energy Commission. [online] Available from: www.climateassessment.ca.gov., 2018.

Prugh, L. R., Deguines, N., Grinath, J. B., Suding, K. N., Bean, W. T., Stafford, R. and Brashares, J. S.: Ecological winners and losers of extreme drought in California, Nat. Clim. Chang., 8(9), 819–824, doi:10.1038/s41558-018-0255-1, 2018.

Quichimbo, E. A., Singer, M. B. and Cuthbert, M. O.: Characterizing groundwater-surface water interactions in idealized ephemeral stream systems, Hydrol. Process., (February), 1–15, doi:10.1002/hyp.13847, 2020.

Reynier, W. A., Hilberg, L. E. and Kershner, J. M.: Southern California Grassland Habitats: Climate Change Vulnerability Assessment Summary, EcoAdapt [online] Available from: http://ecoadapt.org/, 2017.

Roberts, D., Bradley, E., Roth, K., Eckmann, T. and Still, C.: Linking physical geography education and research through the development of an environmental sensing network and project-based learning, J. Geosci. Educ., 58(5), 262–274, doi:10.5408/1.3559887, 2010.

Shukla, S., Safeeq, M., Aghakouchak, A., Guan, K. and Funk, C.: Temperature impacts on the water year 2014 drought in California, Geophys. Res. Lett., 42(11), 4384–4393, doi:10.1002/2015GL063666, 2015.

Singer, M. B. and Michaelides, K.: Deciphering the expression of climate change within the Lower Colorado River basin by stochastic simulation of convective rainfall, Environ. Res. Lett., 12(10), doi:10.1088/1748-9326/aa8e50, 2017.

Singer, M. B., Michaelides, K. and Hobley, D. E. J.: STORM 1.0: A simple, flexible, and parsimonious stochastic

Deleted: Monitor
Formatted: Font colour: Auto, English (UK)
Formatted: Font colour: Auto, English (UK)
Deleted: Natural
Deleted: System Sciences,
Formatted: Font colour: Auto, English (UK)
Deleted: and
Formatted: Font colour: Auto, English (UK)
Formatted: Font colour: Auto, English (UK)
Deleted: Journal of Geophysical Research:
Formatted: Font colour: Auto, English (UK)
Deleted: Journal of
Formatted: Font colour: Auto, English (UK)
Deleted: Environments,
Formatted: Font colour: Auto, English (UK)
Deleted: Nature Climate Change,
Formatted: Font colour: Auto, English (UK)
Deleted: Hydrological Processes,
Formatted: Font colour: Auto, English (UK)
Deleted: Reynier, W. A., Hillberg, L. E. and Kershner, J. M.: Southern California Grassland Habitats: Climate Change Vulnerability Assessment Synthesis, EcoAdapt, Version 1., 2016.¶
Formatted: Font colour: Auto, English (UK)
Deleted: Journal of Geoscience Education,
Formatted: Font colour: Auto, English (UK)
Deleted: Rosolem, R., Gupta, H. V., Shuttleworth, W. J., de Gonçalves, L. G. G. and Zeng, X.: Towards a comprehensive approach to parameter estimation in land surface parameterization schemes, Hydrological Processes, 27(14), 2075–2097, doi:10.1002/hyp.9362, 2013.¶
Formatted: Font colour: Auto, English (UK)
Deleted: Geophysical Research Letters,
Formatted: Font colour: Auto, English (UK)
Deleted: Environmental Research Letters,
Formatted: Font colour: Auto, English (UK)

rainfall generator for simulating climate and climate change, Geosci. Model Dev., 11(9), 3713–3726, doi:10.5194/gmd-11-3713-2018, 2018.

Singh, M. and Meyer, W. M.: Plant-soil feedback effects on germination and growth of native and non-native species common across Southern California, Diversity, 12(6), doi:10.3390/D12060217, 2020.

Small, E. E., Roesler, C. J. and Larson, K. M.: Vegetation response to the 2012-2014 California drought from GPS and optical measurements, Remote Sens., 10(4), 1–16, doi:10.3390/rs10040630, 2018.

Swain, D. L., Tsiang, M., Haugen, M., Singh, D., Charland, A., Rajaratnam, B. and Diffenbaugh, N. S.: The Extraordinary California Drought of 2013/2014: Character, Context, And The Role Of Climate Change, Am. Meteorol. Soc., (September), 2014.

Thomas, B. F., Famiglietti, J. S., Landerer, F. W., Wiese, D. N., Molotch, N. P. and Argus, D. F.: GRACE Groundwater Drought Index: Evaluation of California Central Valley groundwater drought, Remote Sens. Environ., 198, 384–392, doi:10.1016/j.rse.2017.06.026, 2017.

Thorne, J. H., Boynton, R. M., Holguin, A. J., Stewart, J. A. . and Bjorkman, J.: A climate change vulnerability assessment of California's terrestrial vegetation., 2016.

Trenberth, K. E.: Changes in precipitation with climate change, Clim. Res., 47(1–2), 123–138, doi:10.3354/cr00953, 2011.

Westerling, A. L. and Bryant, B. P.: Climate change and wildfire in California, Clim. Change, 87(1 SUPPL), doi:10.1007/s10584-007-9363-z, 2007.

Westerling, A. L., Hidalgo, H. G., Cayan, D. R. and Swetnam, T. W.: Warming and earlier spring increase Western U.S. forest wildfire activity, Science (80-.)., 313(5789), 940–943, doi:10.1126/science.1128834, 2006.

Westra, S., Fowler, H. J., Evans, J. P., Alexander, L. V., Berg, P., Johnson, F., Kendon, E. J., Lenderink, G. and Roberts, N. M.: Future changes to the intensity and frequency of short-duration extreme rainfall, Rev. Geophys., 52(3), 522–555, doi:10.1002/2014RG000464.Received, 2014.

Wilkening, J., Pearson-Prestera, W., Mungi, N. A. and Bhattacharyya, S.: Endangered species management and climate change: When habitat conservation becomes a moving target, Wildl. Soc. Bull., 43(1), 11–20, doi:10.1002/wsb.944, 2019.

Williams, A. P., Seager, R., Abatzoglou, J. T., Cook, B. I., Smerdon, J. E. and Cook, E. R.: Contribution of anthropogenic warming to California drought during 2012 – 2014, Geophys. Res. Lett., 42, 6819–6828, doi:10.1002/2015GL064924.Received, 2015.

Williams, A. P., Abatzoglou, J. T., Gershunov, A., Guzman-Morales, J., Bishop, D. A., Balch, J. K. and Lettenmaier, D. P.: Observed Impacts of Anthropogenic Climate Change on Wildfire in California, Earth's Futur., (7), 892–910, doi:10.1029/2019EF001210, 2019.

Deleted: Geoscientific
Deleted: Development,
Formatted: Font colour: Auto, English (UK)
Formatted: Font colour: Auto, English (UK)
Deleted: Sensing,
Formatted: Font colour: Auto, English (UK)
Deleted: American Meteorological Society,
Formatted: Font colour: Auto, English (UK)
Deleted: Sensing of Environment,
Formatted: Font colour: Auto, English (UK)
Formatted: Font colour: Auto, English (UK)
Deleted: Climatic
Formatted: Font colour: Auto, English (UK)
Deleted: ,
Formatted: Font colour: Auto, English (UK)
Formatted: Font colour: Auto, English (UK)
Deleted: Wildlife Society Bulletin,
Formatted: Font colour: Auto, English (UK)
Deleted: Geophysical Research Letters,
Formatted: Font colour: Auto, English (UK)
Deleted: Future,
Formatted: Font colour: Auto, English (UK)

Wilson, S. D., Schlaepfer, D. R., Bradford, J. B., Lauenroth, W. K., Duniway, M. C., Hall, S. A., Jamiyansharav, K., Jia, G., Lkhagva, A., Munson, S. M., Pyke, D. A. and Tietjen, B.: Functional Group, Biomass, and Climate Change Effects on Ecological Drought in Semiarid Grasslands, J. Geophys. Res. Biogeosciences, 123(3), 1072–1085, doi:10.1002/2017JG004173, 2018.

Xiao, M., Koppa, A., Mekonnen, Z., Pagán, B. R., Zhan, S., Cao, Q., Aierken, A., Lee, H. and Lettenmaier, D. P.: How much groundwater did California's Central Valley lose during the 2012–2016 drought?, Geophys. Res. Lett., 44(10), 4872–4879, doi:10.1002/2017GL073333, 2017.

Deleted: Journal of Geophysical Research:

Formatted: Font colour: Auto, English (UK)

Deleted: Geophysical Research Letters,

Formatted: Font colour: Auto, English (UK)

Formatted: Font colour: Auto

Author Contributions:

Conceptualization: MBS,MOC,KC,DR,JS

Methodology: MMW,MBS,MOC

Data Curation: MMW,RS

Formal analysis: MMW,RS

Writing – Original Draft: MMW

Writing – Review & Editing: MMW,MBS,MOC,KC,DR,JS,RS

Acknowledgments and Data

This work was supported by The National Science Foundation (BCS-1660490, EAR-1700517 and EAR-1700555) and the Department of Defense's Strategic Environmental Research and Development Program (RC18-1006). We thank D. Roberts for providing the IDEAS data set, which is publicly available at http://www.geog.ucsb.edu/ideas/. MOC gratefully acknowledges funding for an Independent Research Fellowship from the UK Natural Environment Research Council (NE/P017819/1).

The authors declare that they have no conflict of interest.

Formatted

Deleted: Page Break

Page 4: [1] Deleted Maria Magdalena Warter 12/03/2021 10:01:00

Page 4: [2] Deleted Maria Magdalena Warter 12/03/2021 10:01:00

Page 4: [3] Deleted Maria Magdalena Warter 12/03/2021 10:01:00

Page 7: [4] Deleted Maria Magdalena Warter 12/03/2021 10:01:00

Page 7: [5] Deleted Maria Magdalena Warter 12/03/2021 10:01:00

Page 11: [6] Deleted Maria Magdalena Warter 12/03/2021 10:01:00

Page 11: [7] Deleted Maria Magdalena Warter 12/03/2021 10:01:00

Page 19: [8] Deleted Maria Magdalena Warter 12/03/2021 10:01:00

Page 19: [8] Deleted Maria Magdalena Warter 12/03/2021 10:01:00

Page 19: [8] Deleted Maria Magdalena Warter 12/03/2021 10:01:00

Page 19: [8] Deleted Maria Magdalena Warter 12/03/2021 10:01:00

Page 19: [8] Deleted Maria Magdalena Warter 12/03/2021 10:01:00

Page 19: [8] Deleted Maria Magdalena Warter 12/03/2021 10:01:00

Page 19: [8] Deleted **Maria Magdalena Warter** **12/03/2021 10:01:00**

Page 19: [8] Deleted **Maria Magdalena Warter** **12/03/2021 10:01:00**

Page 19: [8] Deleted **Maria Magdalena Warter** **12/03/2021 10:01:00**

Page 19: [8] Deleted **Maria Magdalena Warter** **12/03/2021 10:01:00**

Page 19: [8] Deleted **Maria Magdalena Warter** **12/03/2021 10:01:00**

Page 19: [8] Deleted **Maria Magdalena Warter** **12/03/2021 10:01:00**

Page 19: [8] Deleted **Maria Magdalena Warter** **12/03/2021 10:01:00**

Page 19: [8] Deleted **Maria Magdalena Warter** **12/03/2021 10:01:00**

Page 19: [8] Deleted **Maria Magdalena Warter** **12/03/2021 10:01:00**

Page 19: [8] Deleted **Maria Magdalena Warter** **12/03/2021 10:01:00**

Page 19: [8] Deleted **Maria Magdalena Warter** **12/03/2021 10:01:00**

Page 19: [8] Deleted Maria Magdalena Warter 12/03/2021 10:01:00

Page 19: [8] Deleted Maria Magdalena Warter 12/03/2021 10:01:00

Page 19: [8] Deleted Maria Magdalena Warter 12/03/2021 10:01:00

Page 19: [9] Deleted Maria Magdalena Warter 12/03/2021 10:01:00

Page 19: [10] Deleted Maria Magdalena Warter 12/03/2021 10:01:00

Page 19: [10] Deleted Maria Magdalena Warter 12/03/2021 10:01:00

Page 19: [10] Deleted Maria Magdalena Warter 12/03/2021 10:01:00

Page 19: [10] Deleted Maria Magdalena Warter 12/03/2021 10:01:00

Page 19: [10] Deleted Maria Magdalena Warter 12/03/2021 10:01:00

Page 19: [11] Deleted Maria Magdalena Warter 12/03/2021 10:01:00

Page 19: [11] Deleted Maria Magdalena Warter 12/03/2021 10:01:00

Page 19: [12] Deleted Maria Magdalena Warter 12/03/2021 10:01:00

Page 19: [12] Deleted Maria Magdalena Warter 12/03/2021 10:01:00

Page 19: [12] Deleted Maria Magdalena Warter 12/03/2021 10:01:00

Page 19: [12] Deleted Maria Magdalena Warter 12/03/2021 10:01:00

Page 19: [12] Deleted Maria Magdalena Warter 12/03/2021 10:01:00

Page 19: [12] Deleted Maria Magdalena Warter 12/03/2021 10:01:00

Page 19: [12] Deleted Maria Magdalena Warter 12/03/2021 10:01:00

Page 19: [12] Deleted Maria Magdalena Warter 12/03/2021 10:01:00

Page 20: [13] Deleted Maria Magdalena Warter 12/03/2021 10:01:00

Page 25: [14] Deleted Maria Magdalena Warter 12/03/2021 10:01:00

Page 25: [15] Deleted Maria Magdalena Warter 12/03/2021 10:01:00